



INAOE

**INSTITUTO NACIONAL DE ASTROFÍSICA, ÓPTICA
Y ELECTRÓNICA.**

**Construction of a Light Sheet system with novel
illumination configurations**

by

Lic. Rodrigo Itzamná Becerra Deana

A thesis submitted as a requirement for the degree of

MASTER IN OPTICS

Thesis advisor:

Dr. Pablo Loza Álvarez- ICFO

Dr. Rubén Ramos García - INAOE

Sta. María Tonantzintla, Puebla, México

©INAOE 2019

Derechos Reservados

El autor otorga al INAOE el permiso de reproducir
y distribuir copias de esta tesis en su totalidad o en
partes mencionando la fuente.



Abstract

Light Sheet Fluorescence Microscopy is a highly efficient technique (in terms of excitation and detection of the signal) to observe, in high resolution (x, y and z), living samples. It works by illuminating the sample with a light sheet, normally produced using a cylindrical lens. The generated fluorescence signal is recorded in a perpendicular way to the light sheet. Until now, LASERS, considered as point sources, had to be used to ensure the production of a thin light sheet. In this project, I present a new way to create a Light Sheet using LEDs or any extended source in general in combination with the use of a Photonic Lantern (PL). This has the advantage that they will produce a more homogenous illumination, have a large bandwidth, produce no speckle or any interference patterns and is not expensive. Thus, in this work, I will introduce the working principle of the Light Sheet Fluorescence Microscope (LSFM), then I will show the different kind of sources of light to generate a Light Sheet, including the use of extended sources. Then I will explain the Photonic Lantern, its constructions, and its characterization. This allows to present, for the first time, the combined use of a PL with an extended source for obtaining high-resolution images in a light sheet microscope. Finally, I will show the use of LEDs and PL as the ideal tool to produce high-resolution images of non-fluorescently labeled samples using elastic scattering as a contrast mechanism. Importantly, this opens up a new range of applications in which fluorescence signal is too weak (for example for fast imaging) or for conditions in which labeling is not possible at all.

Acknowledgments

Agradezco a mis padres, hermanos, abuela y familiares, personas especiales para mí, amigos y todos los que han estado presentes en mi crecimiento personal y profesional como científico para llegar a ser la persona que hoy soy y cumplir mis objetivos.

En especial, quiero agradecer a Jordi Andilla por sus enseñanzas durante mi proyecto de tesis, a mi asesor Rubén Ramos por su apoyo durante la realización del proyecto, Sara González, Vittoria Finazzi, Laurent Ladépêche, Gustavo Castro, Pablo Loza y al grupo de SLN, por su apoyo, ánimos y ayuda para realizar este gran proyecto de tesis.

Por último, quiero agradecer al CONACYT, INAOE e ICFO por financiar y permitirme realizar con éxito mis estudios de Maestría.

“Esta investigación fue realizada gracias al apoyo del Consejo de Ciencia y Tecnología del Estado de Puebla”.

Dedication

To everyone that helped me and supported me to achieve this goal.

Table of Contents

Abstract.....	iii
Acknowledgments	iv
Dedication.....	vi
Table of Contents.....	vii
Chapter 1: Statement of the Problem	1
Objective.....	2
Methodology.....	3
Chapter 2: Light Sheet Fluorescence Microscopy	5
Microscopy	5
Illumination	10
Detection.....	13
Mounting	17
Complete System.....	18
Chapter 3: Light sources.....	24
Characteristics of a Laser	24
Setup with a LASER	26
Characteristics of a LED	28
Setup with a LED.....	30
Comparison.....	32
Chapter 4: Photonic Lanterns	34

Optical fibers and the Photonic Lantern	34
Physical Properties	37
Design of a Photonic Lantern.....	42
Photonic Lanterns with an extended source.....	47
Comparison of an optical fiber and a Photonic Lantern.....	51
Chapter 5: Light sheet with photonic lanterns	53
Usage of PL in LS	53
Characteristics of the LS in PL.....	57
Comparison with standard LSFM	58
Three color imaging and Scattering	65
Chapter 6: Conclusions and future work	70
Appendix.....	71
Program to control the acquisition of images	71
Program to the chiller.....	72
Making a Photonic Lantern.....	73
Details of a extended source with a PL	79
Details of mounting a PL in a LSFM.....	81
Zebrafish immunostaining.....	82
List of Tables.....	84
List of Figures	85
Bibliography.....	92

Chapter 1: Statement of the Problem

Microscopy is a powerful tool to study cells. To obtain the right conclusions during observing and monitoring the cells, these need to be in a natural environment, considering the three space dimensions. For that, the acquisition of 3D images of living samples and its behavior is fundamental for the research in biomedical areas. One of the microscopy techniques that allows imaging the evolution of cells in their environment and 3D in an easy way is light sheet fluorescence microscopy (LSFM).

LSFM is a relatively new technique that uses a laser in an orthogonal axis to the detection direction to produce the imaging, having the focused light in a plane and not in a point. This technique also allows for a faster visualization technique, producing low photodamage and low photobleaching to the sample, these characteristics contribute to LSFM as an efficient illumination and detection method, having an optical sectioning of the sample for every illuminated plane. Also, using fluorescence markers LSFM can show specific structures of the sample

Furthermore, these aspects show that Light Sheet Fluorescent Microscope is an efficient tool in microscopy, to focus light in a line or a plane in thickness between $\sim 1\text{-}5\ \mu\text{m}$. Until now, the light source used in LSFM are lasers, but thinking that we are focusing in a “plane” and not in a point, it could be possible to create a light sheet with an extended source, manipulating the shape of the output light to a plane. This could be not so efficient in term of power of the source, but in microscopy, you require low power. Also with this efficient illumination and detection, some microwatts power will be enough to do imaging.

As an extended source cannot be focused on points or planes, several ways have been devised to achieve it, but nowadays, there is an optical tool to modify the

shape and the behavior of the light, which is the Photonic Lantern (PL), which will help to create a Light Sheet with incoherent light.

Then, the light from an extended source into a light sheet, then we can consider the use of Light Emitting Diodes (LED) for LSFM. One of the most important improvement is the imaging scattering, which can be created because the incoherent light will not have patterns of speckle. Having a novel non-invasive illumination technique, will allow us to observe a sample in its natural environment.

This tool could be the way to avoid the lasers in light LSFM which could become to be the cheapest technique to do high resolution microscopy.

Objective

The main objective is to build a light sheet fluorescence microscope with an incoherent light or extended source and still produce images with high resolutions.

Specific objectives

To demonstrate this challenging objective, specific tasks need to be performed.

- Build a light sheet fluorescence microscope and characterize it.
- Construction, characterization and use of a PL
- Implement a PL in the LSFM.
- Characterization of the full system
- Observation of biological samples.
- Image acquisition

Methodology

To achieve the aforementioned tasks, there are some steps to reach the goal. Understand the characteristics of a light sheet fluorescence microscope.

- Assembly of a LSFM.
- Testing it experimentally.
- Image capture and creation of fast 3D images.

The second part is to implement an extended source and the LED. To identify the system losses and the sizes of the light sheet that it is possible to create with this new device.

- Characteristic of a laser.
- Light Sheet Fluorescence Microscopy with a Laser.
- Characteristic of an extended source.
- Light Sheet Fluorescence Microscopy with an extended source.
 - State of the art.
 - Previous results.
 - Characteristics of this setup.
- Comparison.

Next step consists of building the PL and characterize its performance with an extended source coupled to it.

- Choosing the material to create the PL.
- Create of the PL.
- Characterization of the PL

This characterization and creation of the PL involves the operation of several equipments.

The final part is the implementation of the photonic lantern in the light sheet microscope.

- Mount the new device in a Light Sheet Fluorescence Microscope.
- Characteristics of the setup with the Photonic Lantern.
 - Sources of Losses.
- Characterization of the light sheet.
- Acquisition of images.
- Comparison.
- Creation of an image with more than one channel

Chapter 2: Light Sheet Fluorescence Microscopy

This chapter will explain what is Light Sheet Fluorescence Microscopy, its development, advantages and its principal components. In addition, the chapter explains how to create a Light Sheet Fluorescence Microscope, its characteristics and the data acquisition as a reference to the technique for future chapters.

Also, axial and transversal resolution are mentioned in three sections: illumination, detection and complete system; in each section, resolutions are different due to their specific and different characteristics.

Microscopy

Microscopy is the research area focused on the understanding of the microscopic and mesoscopic world with a scale of nanometers to micrometers. This study involves the behavior, structure, and composition of samples. The microscope's invention was around 1590 by Antonj van Leeuwenhoek, who was the first one registered in the literature [1]. Since those years, the study of the microscopic world started to be divided into many fields of science, including biology and medicine.

In both, it is important to use model organisms to extrapolate their behavior to a human being. Some examples include; “how brain function relies on the communication between large populations of neurons across multiple brain areas in zebrafish” [2] or “detailed information about the inner landscape of tumors, which can improve cancer diagnosis and therapy” [3].

Because most cells are too small to be seen by the naked eye, the study of cells has depended on a great extent on the use of microscopes and consequently, the use of these systems increased the development of optical devices. The main goal of fluorescence microscopy is to visualize specific structures of an organism. The essence of these type of microscope relays in producing fluorescence for generating contrast, with the help of a marker. To excite the marker, a light source

produces an electronic transition between the ground state and the excitation state. After the excitation wavelength, a non-radiative transition occurs, generating fluorescence as a result [4](Figure 1). On the other hand, the labeling is not in the entire sample, it will be attached to a specific molecule, marking the cells containing it, which will give a specific structure, in both senses molecular and density [5]. This leads us to the important question of which type is the right one to use.

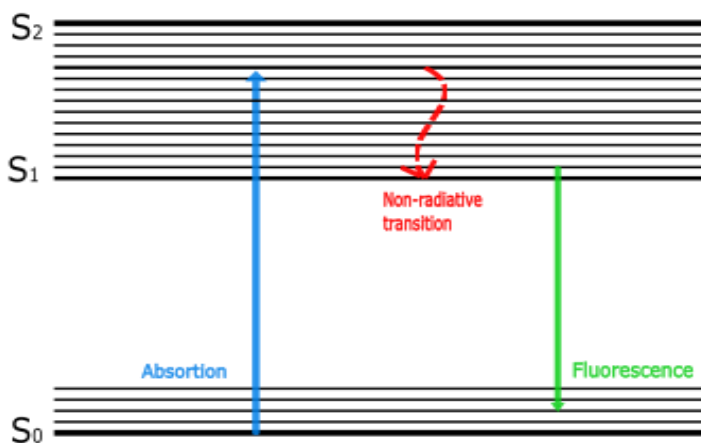


Figure 1 Jablonski's diagram, transitions of energy to obtain fluorescence. The blue line is the level transition of the electron, it happens when the electron is irradiated with the excitation wavelength. The red line represent the non-radiative transition, which the electron lose energy without emitting a photon. The green line is the transition from an excited state to a lower state, emitting in a bigger wavelength than the excitation.

When working with biological samples *in vivo*, three effects have to be considered: Photobleaching, phototoxicity and cell death [6, 7] Photobleaching occurs when the sample is exposed too long time to its excitation wavelength, affecting the dye, ending up by producing no more fluorescence. Phototoxicity is the damage caused by a chemical reaction in the irradiated area. Photobleaching and phototoxicity could both lead to cell death. To avoid those phenomena, it is important to consider that life on Earth is adapted to the solar flux, which is less than 1.4 kW/m². Hence, irradiance on the mounted specimen should not exceed values larger than 1 nW/μm² or 2100 mW/cm² [8].

Some microscopes that work with fluorescence for alive samples are the wide field fluorescence microscope (Figure 2a), the confocal microscope (Figure 2b) and the Light Sheet Fluorescence Microscope (LSFM)(Figure 2c).

The wide field microscope fluorescence is a common microscope with a specific wavelength of illumination to generate fluorescence and a filter to observe the wavelength of emission. In this technique the entire sample is illuminated with the excitation wavelength, producing photobleaching, phototoxicity and cell death in the entire sample. The 3D images are fast and easy to acquire but without optical sectioning (Figure 2a)

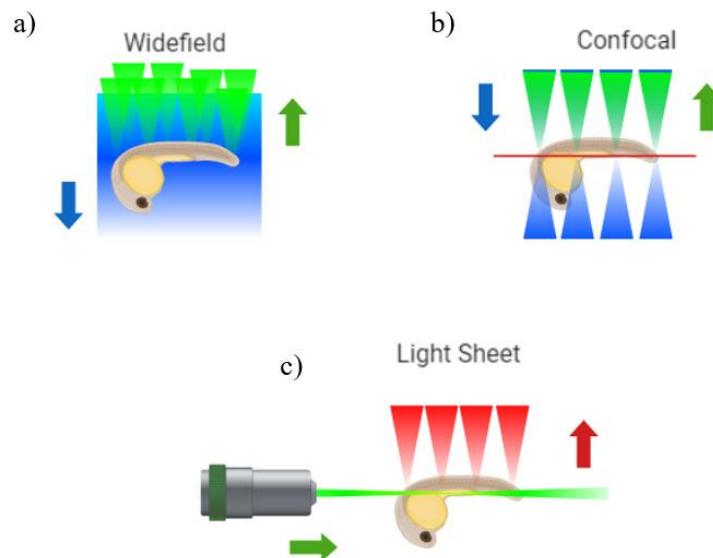


Figure 2 a) Different fluorescence microscopy techniques, a) wide field: illuminating the entire sample with the wavelength of excitation. b) Confocal microscope: Focused the illuminated light in a point. c) LSFM: the illumination is in one plane and the detection is in an orthogonal position with respect the illumination.

The confocal microscope focused the light in a point, getting the information from this illuminated part, giving as a result optical sectioning. The sample is irradiated complete, the same irradiation than wide field producing photobleaching and photodamage. In the case of the 3D images, the acquisition of data is slow since the scan is scanned point by point (Figure 2b).

In the case of LSFM, the illumination is in one plane and its detection in an orthogonal axis than the illumination, having an efficient illumination and detection. It generates optical sectioning, irradiating less the sample and obtaining a fast acquisition of 3D images. It takes the advantages of the other two kinds of microscopes and this thesis will talk about this microscopy technique (Figure 2c).

LSFM is a relatively new technique, which first appeared in 1993. Since then, many implementations, having different names have appeared. Examples are Thin-Sheet Laser Imaging Microscope [ref] (2002) and Single (or selective)-Plane Illumination Microscopy with a specific application (2003-2004) [9, 10]Figure 3.

In LSFM, having the efficient illumination illuminating just one plane, the photobleaching and phototoxicity are low [10, 11, 12]. With a light sheet as illumination, the irradiated area will be just the observation plane of the sample. With this technique, we do not irradiate sections that does not give information. An example of this sections can be found (Figure 2b). The confocal technique irradiate several section of the sample to get a point of information. In addition, it does not require a high power to do imaging.

It has an efficient detection for different points but one of them is for high contrast due to the areas that are not illuminated do not give information.

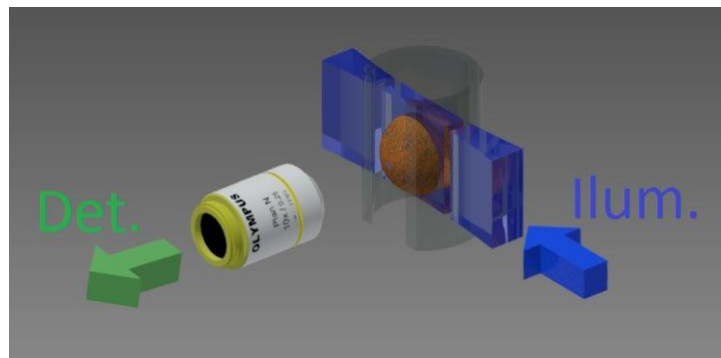


Figure 3 The illumination and detection in LSFM must to be orthogonal due to the plane of focus in the sample.

Focusing the image in the illuminated plane, the data will be collected in 2D having a fast acquisition by moving the sample to create a 3D image. LSFM in comparison

with other techniques, it is one of the fastest to obtain 3D imaging with high-resolution [13, 14, 15, 16], due to, it scans by planes and not point by point like other techniques.

This fast acquisition can be generated with the simplest microscope array, which consists in generate the Light Sheet (LS) with a cylindrical lens and move the sample [17, 18].

Another important fact is the mounting of samples. The light sheet microscope gives an easy way to have more degrees of freedom to illuminate the sample and collect the information. Having the illumination in an orthogonal plane of the detection, there will be a “cube” of space where to put the sample, giving a flexible illumination and detection schemes [13, 14, 19]

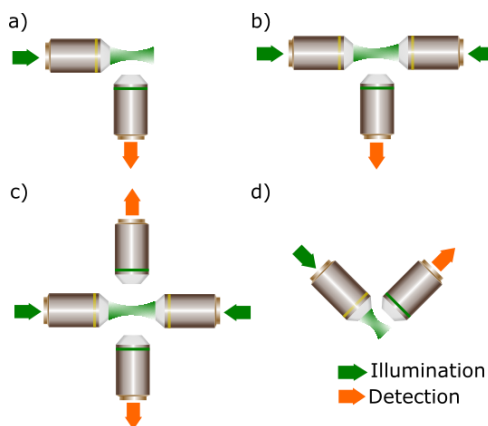


Figure 4 Types of illumination. In microscopy, the different types of illumination depend on the mounting of the set-up. a) The simplest system, one illumination and one detection an orthogonal plane. b) Two illuminations and one detection to have more light in the sample in the same section. c) Two illuminations and two detections. d) Illumination and detection with 45 degrees with respect of the horizontal.

In some cases, the illumination can be double, as shown in Figure 4 b and Figure 4 c. This is to penetrate more and for not having zones without illumination in samples with large thickness [20]. Also, it has double detection to improve the signal, because in the extreme part of the sample the light needs to travel through the entire sample reaching the detection with less power than usual. Having dual detection will be able to observe the other half of the sample. Sometime when the

thickness of the sample is large, in those cases the last part of the sample, the light has to pass through the entire sample, producing a blurred image, to have the image with high resolution from that part, it is important to put another objective. With two detections, the 3D images can be created in two parts, the half with one MO of detection and the other MO will give the information of the other half. Another type of illumination and detection is using the microscope objective with 45° concerning the horizontal; this case is common to use coverslips, to have the traditional mounting of the sample. [21].

Because of the LSFM advantages, such as the low damage in all aspects and fast acquisition, it has been useful for several applications like studies in mouse [22], zebrafish [23], or *C. elegans* [24] just to mention some examples of model organisms. However, it can be improved, because its illumination is with a laser, which produces coherent light. Also, the use of the laser is not necessary, because to work with alive systems, it is necessary to have low power. Using a laser is like trying to use a blowtorch to light a cigar. It has more power than the necessary

Here this thesis presents the first way to do a light sheet with a LED using a Photonic Lantern, proposing a new technique to improve LSFM.

To do that, this work shows how to create the simplest light sheet fluorescent microscope, which is composed of three parts: illumination, detection, and mounting of the sample. It is important to consider that every section must have a point in common that is the location of the sample. Therefore, all the parts will have to match to build just one setup.

Illumination

In the illumination part, the main goal is to create a Light Sheet (LS) for visualizing objects at the microscopy scale. There are several ways to do it, as mentioned in the previous section, and one of the simplest is through a Cylindrical Lens (CL) and a Microscope Objective (MO).

To start, it is important to take into consideration the resolution that is needed for the structure of the cell. The function of the LS is to scan the sample plane by plane. Having a high number of sections of the sample will give a high resolution image. For that reason, it is important to have a LS with a small thickness. Theoretically, the approximate size of the beam can be calculated with two principal equations: Rayleigh range of a beam and paraxial optics theory [25, 26]. The CL focuses one side of the beam that will be collimated with the MO (Figure 5a) and with the other axis the light pass without changing its direction after focused by the MO (Figure 5b).

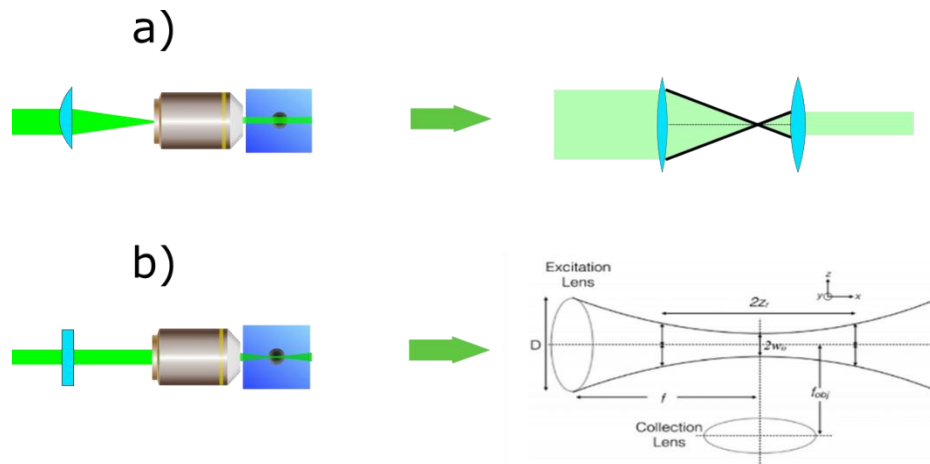


Figure 5 The two axes of the CL. a) The beam is focused in the back focal plane of the MO, generating a collimated beam as a result. b) The axis does not affect the direction of the light and then it will be focused at the work distance.

With these two configurations, we can calculate the size of the LS (in terms of the height, thickness and length). The first one is showed in Figure 5a, which is the height that can be calculated by paraxial optics theory [26], knowing the collimated beam in the entrance, the working distance, the Back Focal Plane (BFP) and the focal length of the lens. As shown in Figure 5a, they have the same angle, therefore making the tangent equal, it gives:

$$\frac{\frac{C1}{2}}{Work\ distance} = \frac{\frac{C2}{2}}{BFP}$$

With as C1 the diameter of the collimated light in the input and C2 in the output, so:

$$BFP \frac{C1}{Work\ distance} = C2$$

As the light will travel collimated in that axis, it will represent the height of the LS. The value of the thickness is calculated with two times the waist of the focused beam [25, 26], also it is named as axial resolution:

$$R_{axial} = 2w_o = \frac{\lambda}{\pi\theta} = 2 \frac{2\lambda f}{\pi D} = 2 \frac{n\lambda}{\pi NA}$$

Where lambda is the wavelength, f is the focal length, D the diameter of the lens, NA is the Numerical Aperture, which is the range of angles that emits or accept light, and it is related to the focal length:

$$NA = n \sin(\theta)$$

$$NA = \frac{f}{D}$$

The last part is the Field of View (FOV) that is two times the Rayleigh range and inversely proportional to the waist [25, 26].

$$FOV = 2Z_r = 2 \frac{\pi w_o^2}{\lambda}$$

In both cases, the NA has an important role, with a high value gives good resolution but with low FOV. Knowing the theoretical values of the LS, the experimental part is to take into consideration those aspects to do it.

The cylindrical lens will determine the height of the LS, which will have to match with the FOV of the camera and the NA will determine the other two aspects, these aspects determine the LS size. In some cases, to require a higher NA's value, it is necessary to use other media; to change the refraction index with is the only value tha can be more than one in the first equation of the NA. Also, it is important to fill all the entrance of the MO to know the real value of the NA, in another case, the Na will be determined for the working distance and the diameter of the circle of

illumination. To illuminate all the entrance of the MO, it must have a telescopic array (Figure 6).

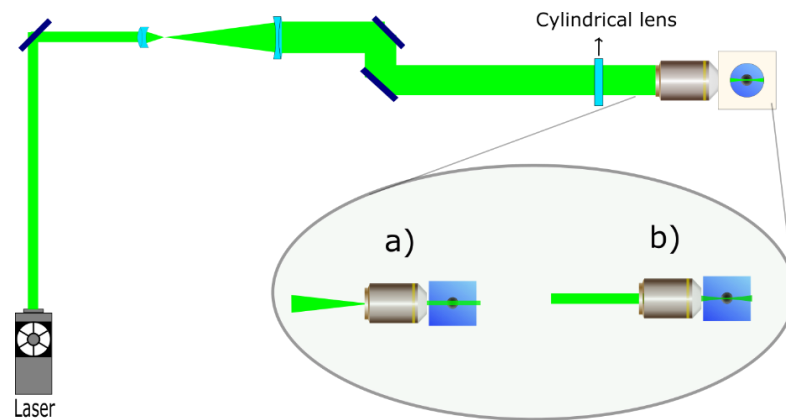


Figure 6 Illumination part in a LSFM filled in the MO. a) Lateral view of the LS in the axis of the CL. b) Upper view, the opposite axis of the CL.

Detection

When the sample is illuminated by light, some phenomena occurred like fluorescence, refraction, speckle, absorption, reflection, scattering, diffuse reflections, between others [27]. This thesis will consider two phenomena to do imaging, the first one is fluorescence, which is used to produce contrast to generate images and the second one is scattering.

As you can see in Figure 7a, a green beam illuminates a sample, which produces irradiation in several wavelengths. One of them is scattering that is generated due to the change of refraction index, which radiation is in the same wavelength. In another case, the molecules absorbed the energy from the illumination beam, which then is irradiated in the form of fluorescence [26] [4]. It is possible to see the scattering in Figure 7b and fluorescence in Figure 7c.

When working with a laser, elastic scattering can be used for generating contrast for producing an image. However, the speckle pattern [26] will be produced scanning the sample, creating a different noise in each image, and the acquired information is a combination of scattering and speckle.

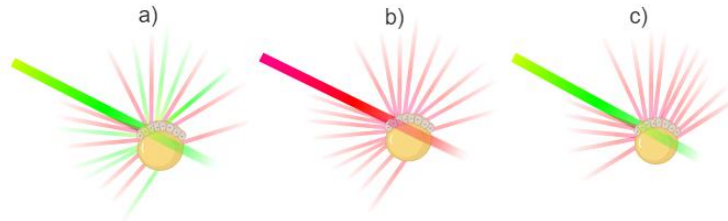


Figure 7 Phenomena in a sample irradiated by a laser. a) Scattering, fluorescence, reflexion, other. b) Scattering. c) Fluorescence

Each way of detection has its advantages for example. For example, fluorescence can provide information about specific structures. However, it implies certain modification of the sample by immunostaining or by the use of genetically modified samples. In contrast, scattering image is easy to do because it requires less power than fluorescence [28]. Another advantage of scattering is that you can produce it with any wavelength. Finally, although it does not need to modify the sample to generate contrast, it has the disadvantage that is not specific for a particular target.

The components of the detection path are a MO, a tube lens, the camera, leaving and the filter (Figure 8). The characteristic of those elements determines the characteristic of our images.

The characteristic of a microscope objective that determines the resolution are the working distance, the NA and the Magnification.

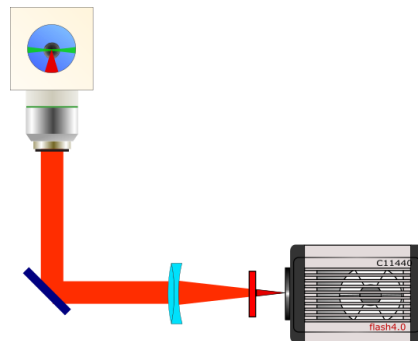


Figure 8 Detection part composed by a microscope objective, a tube lens, filter of the emission wavelength and the camera.

The working distance of the LSFM has to be at the same point that the focused beam of the illumination path, and determines the distance at which we should place the sample. The NA determines the axial resolution in our system, and is defines by the Rayleigh criteria [26]:

$$R_{transversal} = 0.61 \frac{\lambda}{NA}$$

The Rayleigh criteria determine the capability to distinguish two points, where the first minimum of one does not coincide with the maximum of the second one [29]. The resolution in optics is the shortest distance between two points in which we can identify each one. When it is possible to distinguish two points almost together, it is called resolution limit (Figure 9). Taking into consideration that the diffraction limit is the smallest resolution possible, the equation is given by:

$$d = \frac{\lambda}{2 NA}$$

Working with just a “point source”, we can obtain the Point Spread Function (PSF) that is the description of the response of an image to a point source or point object, as well as it gives the resolution of the detection part.

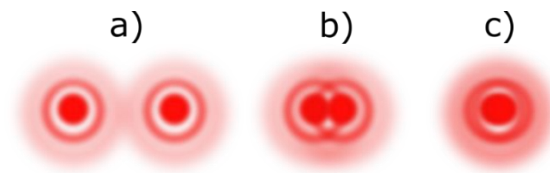


Figure 9 Point sources with diffraction (Airy pattern) separated by different distances. a) Resolved. b) Resolution limit. c) Unresolved

Another resolution related with LS is the axial resolution of the detection which taking into a count the criteria of the Full Width at Half-Maximum (FWHM) that is proportional to $Sinc^2$ function, due to, the Airy pattern [26], leaving the axial resolution as:

$$R_{det-axial} = 1.78 n \frac{\lambda}{NA^2}$$

Where n is the refraction index. Finally, another essential point in which the MO is involved is the magnification, which is either related to the Tube Lens (TL) that its aim to create an image in a plane, before focusing the light coming from the MO to the camera.

The relation among the MO's magnification, the TL's focal length, and the MO's focal length, that is [25]:

$$M = \frac{f_{TL}}{f_{MO}}$$

Where the f_{MO} is given by the manufacturer. One example is Nikon, all its focal length is 200 divided by the magnification of the objective, if there is TL with 200mm of focal length, the magnification will be determined by the MO. Every brand has its focal length so that the magnification will not be the same with different MO and TL. Also, every optical device has to be in the right position.

Having the magnification, it is possible to calculate the FOV. Both are related to [25]:

$$FOV_x = FOV_d / M$$

Where

$$FOV_d = \#pixels_x (Pixel\ size)_x$$

Where x depends on the axis. Using Orca Flash 4.0 Hamamatsu camera, the pixel size is $6.5\mu m$ and in an experiment with 10X of magnification, the size of each point or pixel is $0.65\mu m$ for the 2024 pixels.

Mounting

The essential part here is the sample. It will give the information for media, environment, size, etc. Thus, what will be the labeled structure or the dye illuminated with the specific wavelength, the camera must have the right filter to observe only fluorescence. Here the magnification needs to be specific to observe the required structures.

Equally important is the mounting setup is the degree of freedom that you can control. Figure 10 shows a system that it can move the sample in micro steps in the three axes (x,y,z), also it is possible to rotate the sample to see it in a different point of view. Doing a program LabVIEW facilitates the movement of the motors in micrometers.

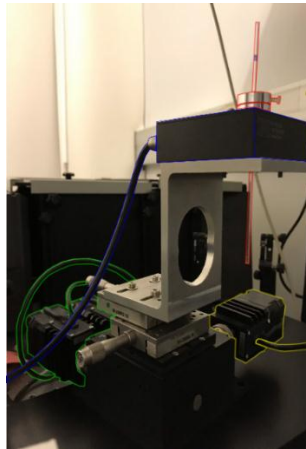


Figure 10 Mounting setup. The red line shows the capillary tube where is mounted the sample, the blue one to control the rotation and the green and yellow one to control the three axis X, Y, and Z.

With this controller of the samples, the most difficult task is to put them in this mounting considering toxicity of the chamber, environment, how to maintain the sample alive, and more. In all the next cases of the thesis, the imaging was performed *in vitro* using agarose to hold the specimens. Important to note is that agarose concentration was selected to have the same refractive index of the water, thus minimizing aberrations. To mount the sample, this was immersed in agarose.

Then this was sucked inside a capillary tube. Once the agarose was solidified, this was pulled outside the capillary tube. In another case, it is possible to introduce the sample with agarose in the Fluorinated Ethylene Propylene (FEP) tube, which has the same refraction index, in this case, the sample was left inside the FEP tube.

Complete System

We started by characterizing the performance of the full mounted system incorporating the illumination, detection and sample mounting components. For that, beads, which are little fluorescent particles in different wavelengths and sizes, were used. To adequately measure the resolution, the beads had to have a size smaller than that calculated for of the LS.

To start the characterization, it is important to know where the focused plane is without the CL and mounting a fluorescent liquid, for example, Sulforhodamine B (SRB), with the wavelength of excitation at 565nm and emission at 586nm. Collocating the right filter, it will show the path of the beam and the focusing part will be the cone of light (Figure 11a). Collocating the CL, the light will cover the entire screen, if the high of the LS fill the entire screen (Figure 11b), in the case that the light is not covering the entire camera, there will be a square with light and two with a darker zone.

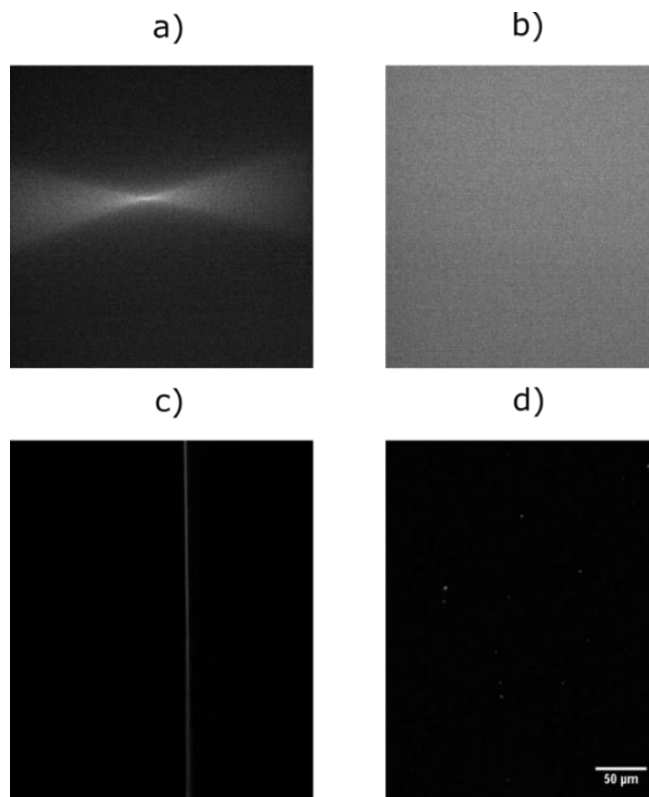


Figure 11 Characteristics of the LS and Beads a) Cone of the focused beam without CL. b) beam with CL in the entire screen. c) Front view Light Sheet. d) Beads.

Collocating a neutral density filter in the optical path and a mirror in the place of the sample, the camera will show the front view of the LS (Figure 11c). To calculate the resolution of the detection, there are many different ways; the most common is by using beads to calculate the PSF, Figure 11d shows some beads, which appear like points in the image. To measure the thickness of the LS and the PSF, it can be calculated with FWHM of Figure 11c and Figure 11d respectively, in ImageJ. To calculate the FWHM of the LS is necessary to move both MO's to find the smallest LS. For the PSF, it can be obtained by doing pixel limited with beads of less size than the LS and applying the FWHM. Nevertheless, for this, it is necessary the real pixel size of the detection, which involves the magnification. To know this characteristic, one way is to take two pictures of the same sample in a known distance in the axis of the propagated light of illumination. Having both images, the next step is to do the maximum projection in ImageJ. The number of

pixels that there are between these two points is equal to the known distance, dividing it between the number of pixels gives the real pixel size and the magnification (Figure 12).



Figure 12 Maximum projection of two images of different distances.

Another essential point where the PSF is involved is in to improve the images because the images are represented like:

$$Image(r) = Object(r) \otimes PSF(r)$$

So, using the deconvolution and dividing:

$$\frac{IMAGE(r)}{PSF(r)} = OBJECT(r)$$

That is the real object. To do that, it requires the PSF to do the deconvolution improving the image as it was the real object.

Having a complete system and its characteristics, the next step is to do imaging. An example of this is Figure 13 with LS around 2um, 0.68 um of pixel size, 488nm of the wavelength of illumination and detection in the range 609nm. For this sample, the best laser was one in the range of 520nm but just to see the imaging, the sample was irradiated with high power. The sample is a cancer spheroid; it is common in LSFM to characterize the system.

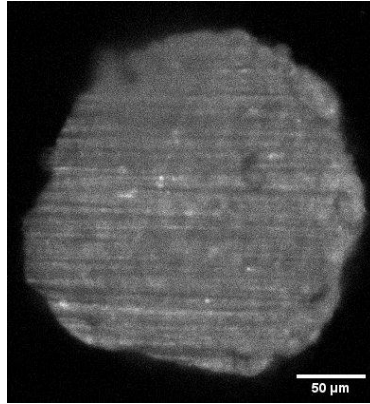


Figure 13 The middle part of a cancer spheroid labeled with H2B-mCherry

For 3D imaging, it is crucial to automatize the system. For that, a software that controls and synchronizes the camera with the motors is essential. There is an example in appendix 1 where there is a diagram of a LabVIEW program to manipulate the samples and take the picture in an automatized way. In some cases, the programs can be done to work without people for several hours to create an image every period.

Taking a sequence of pictures of the sample, the imaging processing could be done in ImageJ with his tools, stacks, and plugging's, to create a 3D image, to see the sample from a different point of view. Figure 14 shows a reconstruction in 3D of two spheroids. The sequence of the image is to show a rotation, to see the front and lateral view. Every picture was taken every 0.9um and it contains around 300 images.

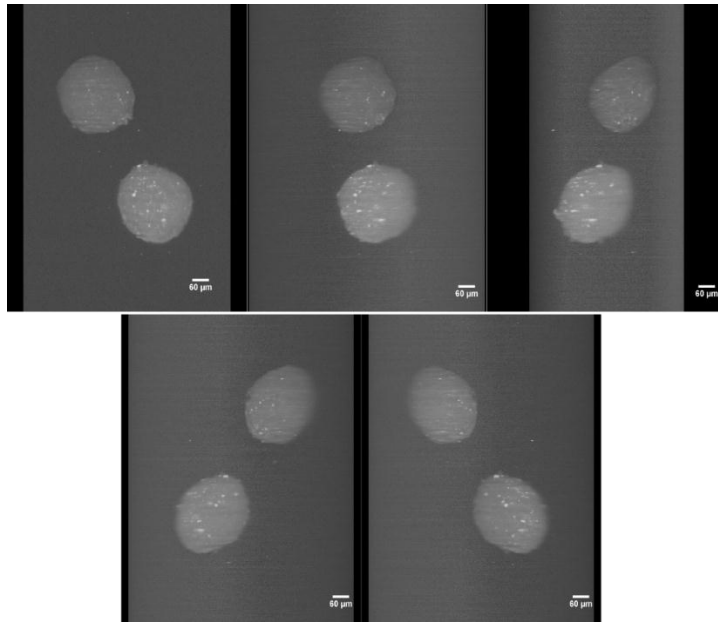


Figure 14 Reconstruction of two spheroids in 3D. All of them are from the same sample in different points of view.

To get more detail and information of the sample it is used the maximum projection of the stack, this is the type of the future images in this thesis. The function is to take the maximum value of each pixel from the images. It looks like Figure 15.

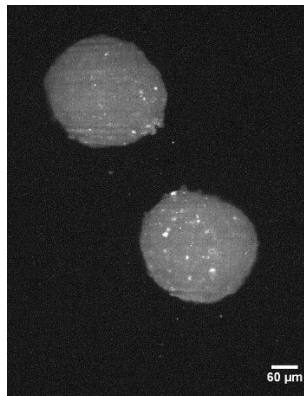


Figure 15 Maximum projection of the two spheroids

These are some typical images and samples in LSFM that can be done building this kind of system. Although there is a good resolution, there are still some limitations with this technique using Laser. The images have some shadow lines, that are from only one source. If there is no fluorescence, the images will have a speckle pattern.

Having this reference, the next step is to know the characteristics of the light sources to find the best parameters to do LSFM, improving the images implementing an extended source using an optical device.

Chapter 3: Light sources

Nowadays, there are several kinds of light sources. One of the most important to develop new techniques for different applications is the laser, being present in several Nobel Prizes. On the other hand, LEDs (or extended sources) have been growing to use them in completely different applications, using them in our daily routine. In this chapter, the main goal is to understand these light sources and how they work with a Light sheet Fluorescence Microscope, to compare the Light Sheet generated from each kind of illumination source, to put in context what is developed now a days and the advantages of each one.

Characteristics of a Laser

A laser is composed by a resonant cavity, a pump source, and an active media, doing population inversion of electrons to generate an amplification of the stimulated emission. For this reason, its name is Light Amplification by Stimulated Emission of Radiation [29]. The characteristics of each laser depend on how it was made. For example, its wavelength, using a specific active media, will give another specific one. This fact leaves several wavelengths in the visible range, infrared and UV.

The wavelength will have a narrow bandwidth that is why it is called monochromatic. In microscopy, that small bandwidth is not a problem because the dyes and fluorophores have a wide excitation bandwidth. With this, as the power increase, also the fluorescence does.

Another characteristic is that the laser is considered as a source point, which cannot be focused in just a point [26], its focused part will have a size, determined by the waist of the beam.

Besides, with this kind of structure beams, we have different modes that can be represented by its light intensity, and those are mathematically represented as an

orthogonal solution of the wave equation [30]. In the case of the lasers, we work with just one mode that is the principal or first one.

Another essential point that is involved in some characteristics is coherence. It has coherence in both senses, spatial and temporal. Therefore, this kind of sources produces interference, which is a phenomenon generated with two identical sources which are coherent, monochromatic and point source. This pattern of bright and dark fringes (Figure 16), this is the superposition of two waves [27].

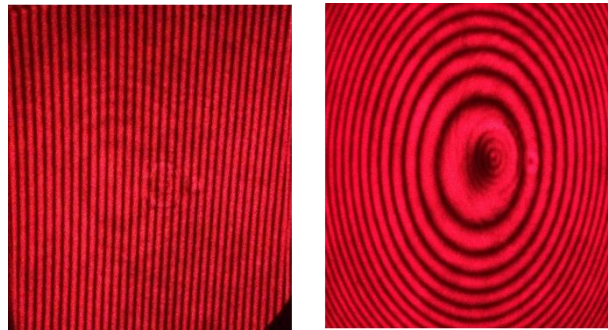


Figure 16 Finger pattern in a Michelson's Interferometer

In the same pattern, considering several point sources produced by diffused reflections, also generate a speckle pattern, which is generated for an irregular surface; here the diffuse reflection sends several rays in all directions, giving a pattern like Figure 17. The last characteristic is the diffraction, which will appear in the smallest size of the LS's thickness with the diffraction limit.

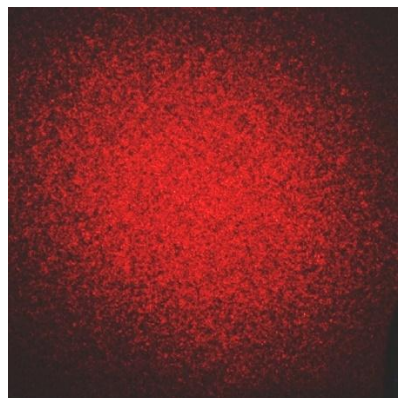


Figure 17 Speckle patterns

Knowing the principal characteristics that appear in this kind of setups will show the disadvantages a LS has with a coherent light.

Setup with a LASER

In a LSFM system (Figure 18), interface and speckle patterns appear because the laser beam passes through all the optical system, sample, the mounting part, and media.

The advantages are the power of the laser, one transversal mode and the spatial coherence of the beam. With that, the focusing of the light can be in a line of 5 μ m or 1 μ m with enough power to do fluorescence. Using an appropriate filter, only the image generated by fluorescence will be detected.

However, for generating an image using elastic scattering, this will be modulated by Interference and speckle. Because, there will be some parts more illuminated than others, the effect of this coherence light will create that pattern since the light touches the sample, producing bright and dark points that pass through the sample illuminating more some parts and some of the speckle pattern will reach the camera. So, the illumination is not homogenous, giving an image with some noise or perturbations. In cases like scattering imaging, speckle will introduce several noises, which will change in every plane of the sample, that is why it cannot remove it.

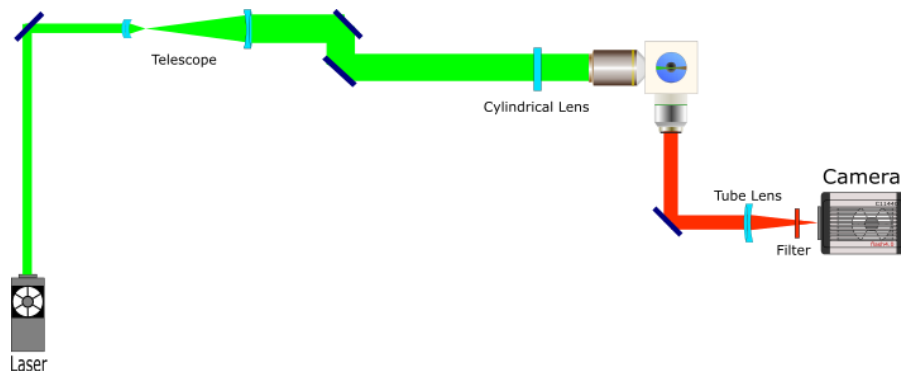


Figure 18 A Light Sheet Fluorescence Microscope

Illuminate more sections or the generation of shadow lines in the images are not a limitation to acquire a good image, that is why it is a useful technique, but it is possible to take more advantage against other microscopes, making some improvements.

An example images obtained using wide field and LSFM are like Figure 19. The first one shows a typical acquisition with wide field, which presents fluorescence and scattering. Figure 19 b represents a section of the sample doing it with LSFM, which has some lines or parts more illuminated than others do. Here some structures are not possible to observe as it has not been fluorescently labeled. With the scattering of the sample, the full structure of the sample appears, giving an extra detail about how it is composed. On the other hand, to have better detail and information for all the focused planes, the maximum projection will give further information.

In wide field, it is not possible to create a 3D image because all the planes give information at the same time, not having contrast and just one plane focused.

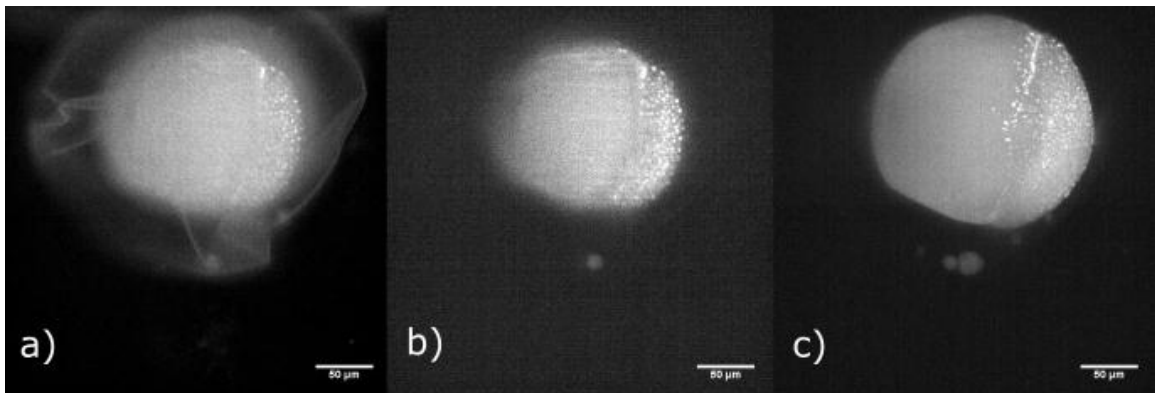


Figure 19 Images of a zebrafish like a sample. a) The bright field in the same position as before one. b) With LSFM. c) Maximum projection of the sample's stack with LSFM

All of this was done with LS around 2 μm , illumination in 488 nm with fluorescence in green. In Figure 19b, there was a filter and the fluorescence always appear. Everything was done using zebrafish eggs.

Those are the kind of sample that is used in biology. It is a model organism, which is used to model pathological conditions, observe behavior of the cells or to study

its growth and if it is possible, to extrapolate the information that could be useful for the human being. To do this kind of application the normal thickness sizes of the LS goes from 1 to 5 μm .

This setup was built to have a reference of the images and a flexible system, in which is possible to change the illumination method.

Characteristics of a LED

LEDs have differences comparing with Lasers in their creation, way of illumination, and characteristics of its behavior. LEDs are considered extended sources. This means that they can be considered as having several point sources. Therefore, these can be considered as objects when working with images in optical systems.

Another characteristic is their high divergence. Therefore, creating a collimated beam is a difficult task. Here is when the losses start to appear. To collect all the light, it is necessary to place a lens in near to the focal length. In some cases, the divergence produces several losses and it cannot be focused in a small area; here, the best option is to collocate the lens in front of the LED. It requires more lenses in short distances to control the light, to try to focus it on the smallest possible image. This is an extended source and it cannot be focused in a point, as the laser does. Each point of illumination of this device will generate its focused point, which put all together will give an extended image. It is important to consider those aspects to have enough power in the output for different applications while trying to obtain the smallest image.

Another essential point is the incoherence in both pathways of the light source. LEDs do not have spatial and temporal coherence, because every point will start to illuminate in a different time and space of the others, changing the phase to a random shape in every part of the space. In addition, the bandwidth is big, for example, Figure 20 shows the spectrum of commercial LEDs that will be shown in the last chapter.

With their behavior, LEDs can no produce interference and speckle in the illuminated sample. Giving some improvements and the possibility to create imaging using elastic scattering as a source of contrast.

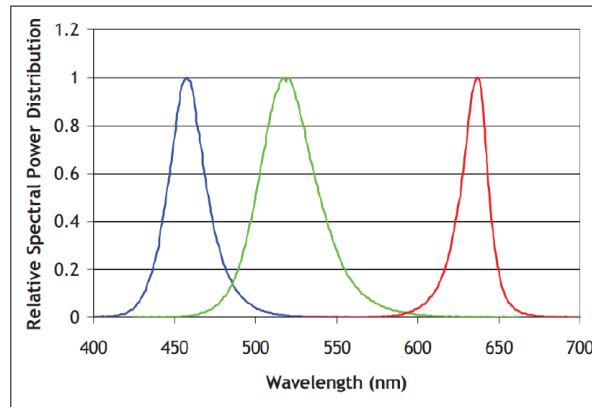


Figure 20 LUMINUS CBT-90 TE LEDs' Spectrum

Although interference is present in this kind of sources, these have a low range of interference when combined in the same optical path. An example is with a Michelson Interferometer, when introducing a collimated white light and fitting the mirrors with the same optical path, the interference pattern will appear but in a small range and the coherent length is small due to the bandwidth.

Another characteristic is the power of the source. Fortunately, LEDs have been growing quickly giving high powers as the same LED mentioned before; it can reach around 10W of power with 13A still being stable. Although it produces high power, there are two problems, first how to collect all the light due to its divergence and second the NA of the lenses.

The last one is the (unknown) high number of modes. Nevertheless, when the light is traveling inside a cavity or waveguide it is possible to calculate the number of modes [26].

Those characteristics are completely different from a laser. In consequence, the generation of thin LS for producing high resolution images becomes difficult.

Setup with a LED

From above we can see that LSM has two principal problems when trying to use a LED as an excitation source: it cannot focus on a point and the divergence of the light. The first one is related to the difficulty in de-magnification of the image of the LED to generate the smallest one, and the second is the power that the sample requires to produce fluorescence.

These problems are not easy to solve, leaving no information in the literature about it. Until now, there is just bright field using LED in microscopy. For that reason, some experiments were performed to have some references for light sheet with incoherent light, to check how to produce it, and to know the limitations.

The first experiment was to illuminate with a collimated light (Figure 21a); trying to do a LS. The result was a LS of 1mm of thickness, in which the images were equivalent conventional bright field as the beam illuminates the entire sample. To reduce it, a diaphragm was implemented (Figure 21b), trying to send enough energy with proper size, giving a LS of 400um. This result in a LS thickness smaller than before but still not useful for microscopy. The third experiment (preliminary results from a former member of the research group), was using a LED with an optical fiber-like waveguide with a large core (CoolLed) Figure 21c). In which you can have a number of modes because it is inside a cavity (Sale), removing the image of the LED. The idea was to collimate the light to create the LS. With that, he did a LS of 40um of thickness reducing it 10 times, but not enough to do LSM.

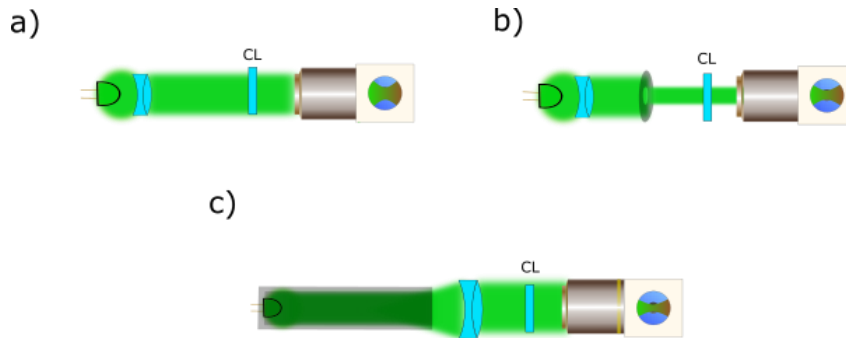


Figure 21 Illumination part of a LSFM. a) Just collimating the light. b) Using a diaphragm. c) LED inside an optical fiber (CL-Cylindrical Lens).

In the three cases, the power is enough to do LS but the sizes of the thickness are large and in the first two cases the image of the LED is produced in the focused plane, just in the third experiment the image of the LED is removed.

To see which one is better, the last experiment was to create a spatial filter (Figure 22). Considering the smallest image that it is possible to produce with a microscope objective and using a pinhole to create the spatial filter, then collimating the light to create the LS. The obtained thickness size was around 20 μm (Figure 23).

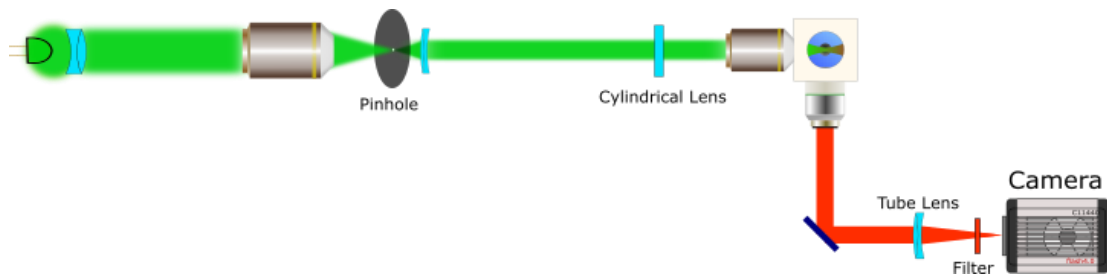


Figure 22 LSFM with incoherent light and a spatial filter (pinhole)

This is the best LS that it is possible create with a LED, a pinhole of 30 μm and lenses. However, it has several losses due to the use of the spatial filter, (small power of the light pass through the pinhole and considering that the divergence produces losses; the power will not be enough to create a fluorescence image). Spatial coherence is one of the principal characteristics to generate a LS with small

thickness, but using a pinhole the losses are incredibly high. In addition, patterns like diffraction and interference will have more opportunity to appear, giving the same problem as before, but with a small length range due to its bandwidth.

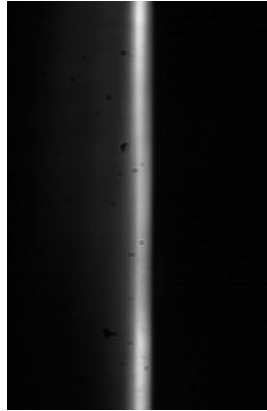


Figure 23 Image of the LS created with incoherent light. It is homogenous and the size is around $20 \mu\text{m}$.

Although this size is the smallest with a LED, it is still too big to do LSFM. In addition, of the need for a complex imaging system (including spatial filter) to properly focus the light. This adds complexity and expenses to a system that still will not produce high resolution images.

To obtain a LSFM with the size of a thickness produced with a laser, the perfect device will have to use both, use only some modes of the LED and to generate spatial filtering.

Comparison

The characteristics of those kinds of sources are different, as Table 1 Shows. Doing LS with coherent light cannot do scattering imaging, the cost is high to change the wavelength, the power is more than enough and with slim spectrum.

By the other side, incoherent light has some improvement in LS, having the opposite characteristics of the laser, obtaining a homogenous illumination, removing interference and the possibility to do scattering imaging. However, the

principal problem is that it is not LSFM; it is bright field, due to, the sizes of the thickness.

The best source or device combined with a source should have the best part of both. To do it, we have to obtain spatial coherence, a low number of modes to improve the focusing to banish the image, enough power, and big bandwidth and with a lower price than a laser.

Characteristics	LASER	LEDs
Kind of source	Point source	Extended source
Bandwidth	Small	Big
Modes	One	multiple
Power	High	medium
Cost	High	Very Low
Interference	High Length Range	Low Length Range
Speckle	Yes	No
Thickness of LS	1~5um	20um

Table 1 Characteristics of a Light Sheet with a Laser and a LEDs

After seeing this comparison, the best idea is to implement a device to modify those mentioned aspects, to obtain a LS with incoherent light. Fortunately, there is a device, which can do exactly that, it is The Photonic Lantern. To understand its behavior, how to implemented and use it, it is necessary to create a LS with a thickness of some micrometers.

Chapter 4: Photonic Lanterns

In this chapter, I am going to introduce the concepts of optical fiber and Photonic Lantern. I will describe its principles, the way to create it and its behavior when used with an extended source. Finally, I will compare the efficiency of collection of a photonic lantern with a bundle of fibers.

Optical fibers and the Photonic Lantern

A waveguide is a device to guide the light. Its principle is based in total internal reflexion, the traveling of light in two materials, one inside the other. The inner material has a higher index refraction than the outer. Following the Snell law and the critical angle [27] when the angle of incidence of light in the interface between the two materials is higher than the critical angle it will undergo total internal reflection and therefore, it will be completely reflected back into the original material. Following this idea, the light can be guided along a material for a certain length with a certain efficiency [26]

The fibre is composed of 3 parts, the core, cladding, and the coating [31]. The first two work like the waveguide and the third one is only a protector of the fiber (Figure 24). In order to inject light into the fibre, the beam has to be parallel to the waveguide or with an angle bigger than the critical one.

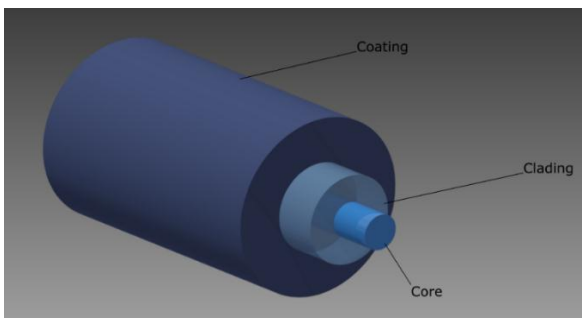


Figure 24 The Optical fiber is composed of three different parts: core and cladding to generate the total internal refraction and the coating to protect the optical fiber.

The core and cladding's refractive index give the Numerical Aperture of the fiber, which is the angle of divergence of the light in the input and output. The NA is given by:

$$NA = \sqrt{n_i^2 - n_o^2}$$

Where n_i is the refractive index of the core and n_o is the refractive index of the cladding.

Also with the NA is possible to calculate the number of modes that travel inside the optical fiber. As it is mention in the previews chapter, the definitions of mode is the transversal solution of the wave equation [26]. Having the NA the other factors that will tells the number of modes that travels in an optical fiber are the diameter and the wavelength, because the number of modes can be calculated as [26]:

$$\text{Number of modes} \approx \frac{4}{\pi^2} \left(2\pi \frac{a}{\lambda_0} NA \right)^2$$

Where a is the radius of the core and λ the wavelength This explains why there are severe optical fiber in the market, depending in the core and the material to have a certain number of modes for each wavelength (Figure 25).

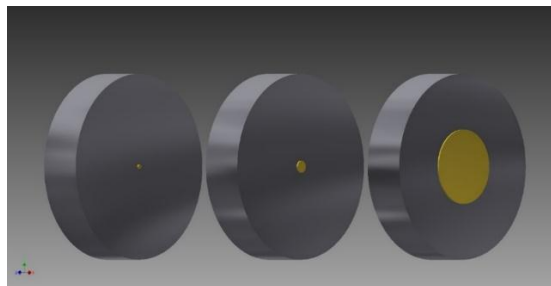


Figure 25 Transversal section of optical fiber: the first one is with a core of 3 μm - size for single mode in around 480 μm , the second one is of 8 μm - single mode in 1550nm and multimode in visible light, the last one 50 μm -multimode for visible light and 1550.

The optical fiber research has been constantly growing, giving new devices with different characteristics to be sensors [32], create lasers [33], telecommunications [34]. One of these devices is the photonic lantern that started in 2005 with

“multimode device with single-mode performance” [35]. *Leon-Saval et al.* gave the principal idea to have a device that change a multimode light to several single modes keeping the possibility to do the opposite transition, starting with several single mode ports and having in the output a multimode performance. The study of PL started since that year but the creation of this kind of devices were with the combiners and fused fiber couplers [36, 37]. In this combiner the principal idea was to mix different wavelengths in only one output. For that, each wavelength had to travel in its own optical fiber. Then each different fiber was fused together to have just one multimode fiber whose output contained all the several wavelengths. This function of the combiner was reported in previous years, being the same idea but with other application [36, 37]. The PL's are made in the same way that it is with two taperings, one to hold the fibers in a capillary tube and the second one to fuse them all [36] .

The tapering in the PL has to be performed to ensure an adiabatic transition. In this way, the decoupling of modes produces low losses, which is the principal objective of a PL. [38]. The adiabatic transition and the decoupling of modes will be explained later in this chapter, as this is one of the principal parts of this project.

The PL has been used before for super-modes in telecommunication [39], filtering [40], or in several functions in astronomy [41], and more [42]. This device started a new field of research for its different applications and its behavior that can be explained with quantum mechanics, having a great impact in different areas. However, there is nothing about the use of PL to produce a collection of single mode outputs starting from an incoherent source for its use in microscopy applications. In the case of this project, this is a new implementation of this device. In particular, we will study PL having different sizes in input diameter and with an, as a proof of concept, we will use as output with fibers with more than just one mode. In particular, the specific case of this work, PL will be used to create a homogeneous light sheet of a few micrometers from an extended source with an improved efficiency.

Physical Properties

A PL works like a “multimode device with single-mode performance” [35], which is composed of three parts; single mode part, a multimode section and the transition tapering fusing the single mode fibers. Normally, the multimode section of the PL is spliced to a multimode fiber, which in this case is not necessary, leaving the device like Figure 26. Then, you can introduce multimode light in the first section and it will give you several single modes in the output to have conservation of energy.

The understanding of the materials will give specific details of the behavior. Also, to make it, there are two necessary materials, optical fibers, and a capillary tube.

For the capillary tube, there are three important aspects: i) the length, ii) the inside diameter, and iii) the refractive index. In case of the length, it has to be enough to do two taperings. This means, a reduction in the size of the capillary tube in all their axis, increasing the length of the capillary tube. Here, the second part involves knowing the inside diameter, where the reduction will hold the fibers. The last one, the refractive index will be present in the second tapering, when the fibers are fused there will be a unified core. In this section, the number of modes will be determined by refraction index of the core and the cladding. The core will be the fusion of the fibers and the capillary tube will be the cladding, which must have a lower refractive index than the core.

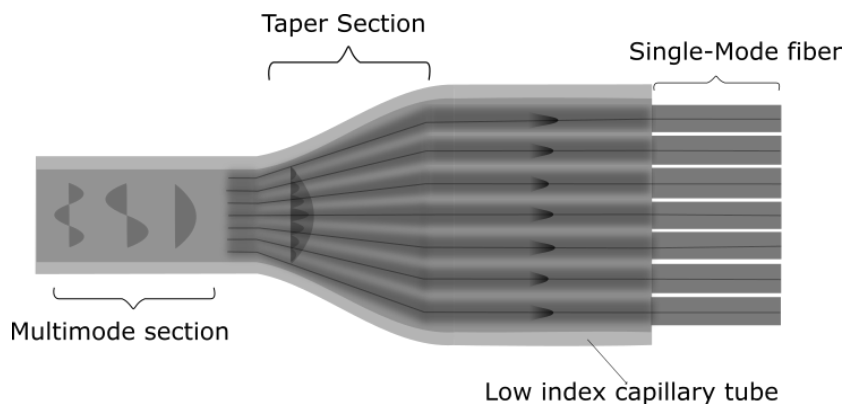


Figure 26 Parts of a Photonic lantern and elements

More importantly, the objective of the capillary tube is to create a waveguide with that new core, and one important parameter is the wavelength, in the inside of the PL. Therefore, to satisfy the boundary conditions to have a waveguide, the capillary tube has to be lower refractive index than the cladding, giving a specific NA [26]:

$$NA = \sqrt{n_i^2 - n_o^2}$$

Having a waveguide, the number of modes inside that cavity will be determined by the V parameter that is involve in the number of modes in optical fibers and their propagation constant, which is [26]:

$$V = 2\pi \frac{a}{\lambda_0} NA$$

Where lambda is the wavelength and a is the ratio of the optical fiber's core. Having the number of modes traveling inside the cavity can be explained with M (the number of modes), which for a large parameter V, the number of modes will be represented as:

$$M \approx \frac{4}{\pi^2} V^2$$

The previous shows that NA plays an important role to obtain the number of modes, but the NA equation is for a homogenous refractive index. This is a problem if in the multimode section are air holes, leaving the fusion of the fiber like a unique option, to keep the equation of the number of modes, the boundary conditions and low losses.

The next section is the tapering, which explains the energy conservation between multimode light to single mode. In order to avoid energy losses, the transition in sizes and melting has to be adiabatic. This means that, under slow or gradually changes, the light will not be able to distinguish that there is any change in its surrounding.

This can also be explained using the adiabatic theorem in quantum mechanics, which refers to situation where the original Hamiltonian of a system can change gradually into a new Hamiltonian that allow the system to adapt its configuration and it will have changes in its probability density in the process [43, 44]. Therefore, this transition is an important part, involving the changing of the refractive index, the distance of each core and its size.

As a result, this gives the transition of a multimode to several single modes. Those transitions of modes give something call super-modes [42]; this name describes the superposition of all the modes in the entrance, providing several single modes in the optical fibers of the output. In the other case, introducing light inside in the optical fibers of the PL, it is possible to create a specific mode in the multimode section.

Considering this process, the modes will work like in Figure 27 Left. The circle number one shows the mode's entrance. In that example, there are two different modes, the number one and the seven. In the circle number two and three, the first mode starts to see the changes, dividing its mode in seven and the seven mode sees that to travel in a better way it has to change its behavior for one simpler. Giving, as a result, the circle number four, where the modes are working together producing several single modes. Finally, each mode travels in its own way, circle number five.

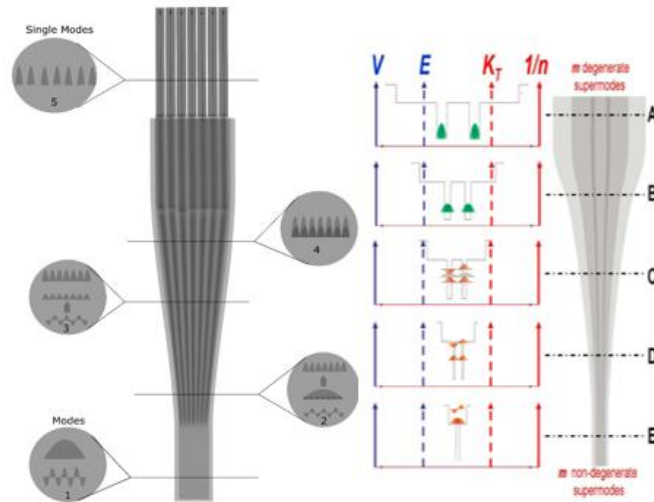


Figure 27. (Left) Transitions of a multimode to single modes. It could start since the number one to number 5 or vice versa. (Right) Schematic evolution of supermodes throughout the tapered transition of the PL. The inverse of the refractive index profile ($1/n$) vs. radius. For the vertical axis, a comparison is made between transverse wavevectors (K_T) of photons and energy of the electron (E) at different positions along with the tapered transition. [45].

This is an adiabatic process, so, it can go in both senses, starting with the number five and finishing with the number one. Considering this option, you can generate modes if you change the optical path, giving in the output a different number of modes or changing it.

For example, splicing several single mode fibers of two PL with the same characteristics, but changing their length of some of the single-mode fibers, it is possible to generate new kind of modes, as there will be a change in the optical path. Other case is changing the sizes of the optical fibers to have more than one mode, having different diameters [38]. So, the input entrance does not have to be the same as the output of the last PL.

All this process can be explained in terms of quantum mechanics. One specific example consists on working with potential wells (Figure 27 right). In reference [45], they explain how changing the properties of the well, the modes will change, this is either changing the Hamiltonian and the eigenvectors. In the case of the PL, the well will change due to the refractive index, the cores' ratio, the sizes and the distance between cores giving a change in the energy and wave vectors.

Another analogy is having a potential well and creating little steps with perturbation theory, until a barrier in the middle of two potential wells is formed. Remembering that this process has to be performed slowly or gradually, it could be done by generating steps with small thickness in the same place, achieving a Dirac's delta between them, producing new solutions in the system, thus, one potential well will change into two.

The last things involved in this transition (Figure 26) are the optical fibers because the adiabatic process will keep the energy of the mode or the number of them, which has a relation with the number of fibers. As you can see in the examples, if we have the seven mode, it will give seven singles modes. However, if there are nine modes it will have losses because it does not have more output ports in which the light can travel.

To have the same energy in the input and the output, the PL must have the same number of fibers than the number of modes [40, 46]. Here again, the capillary tube characteristics play an important role to determine the modes that the fiber can hold. All this process gives, as a result, a transition of a multimode light to several single modes. There are several simulations about it Figure 28 [42], where the number of modes of the PL depends in the characteristics mentioned in this section.

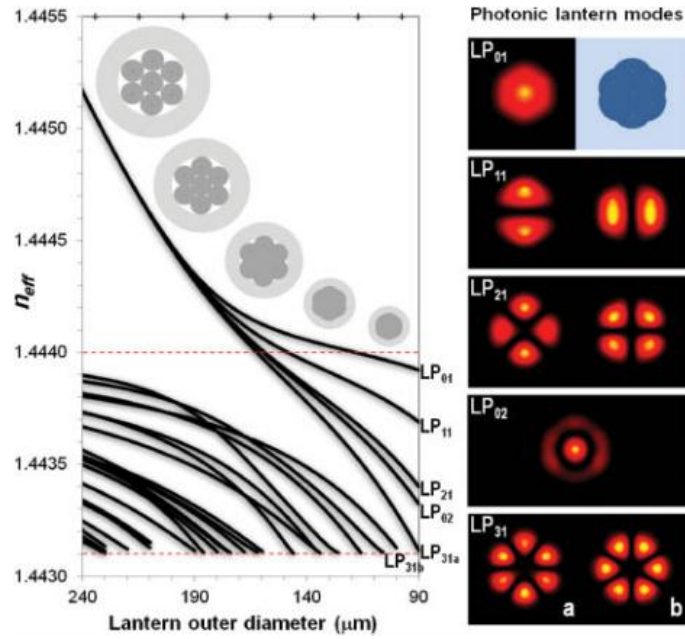


Figure 28 The evolution of modes throughout a seven fiber photonic lantern. The red horizontal dashed lines indicate the core and cladding index of the final multimode core ($n_{co}=1.444$; $n_{cl}=1.4431$). (Right panel) Detail of the calculated modes supported by the photonic lantern at the multimode end. [42]

Design of a Photonic Lantern

The next PL will have seven modes, this is the simplest design where it is possible to see its behaviors and the creation of complex systems will be just an extension of this project.

The materials to create a PL are the optical fibers and the capillary tube. Starting with the capillary tube, which must have a specific refractive index; it can be calculated with the next approximation [47]:

$$NA \approx \frac{\lambda \sqrt{M}}{\pi a}$$

Where all the parameters are known including the NA resulting from the refractive index of the core and cladding fused:

$$\sqrt{n_i^2 - n_o^2} = \frac{\lambda\sqrt{M}}{\pi a}$$

It is worth to notice that the two taperings of the process will affect the final result. So, the design has to involve the relation between them. (Figure 29). The first tapering has to take into consideration the second one, which must have a considerable section to do the melting.

To find the parameters for the first tapering, the design was adapted of 7 fibers in the paper [48], in which the authors worked with 19 single mode fibers. This tapering was made with a Vytran equipment. Having the first tapering, the following step is to introduce the fibers previously soaked with ethanol. This substance cleans them and puts all the fibers together by capillary force to introduce the fibers at the same time in the capillary tube after first tapering (Figure 29).

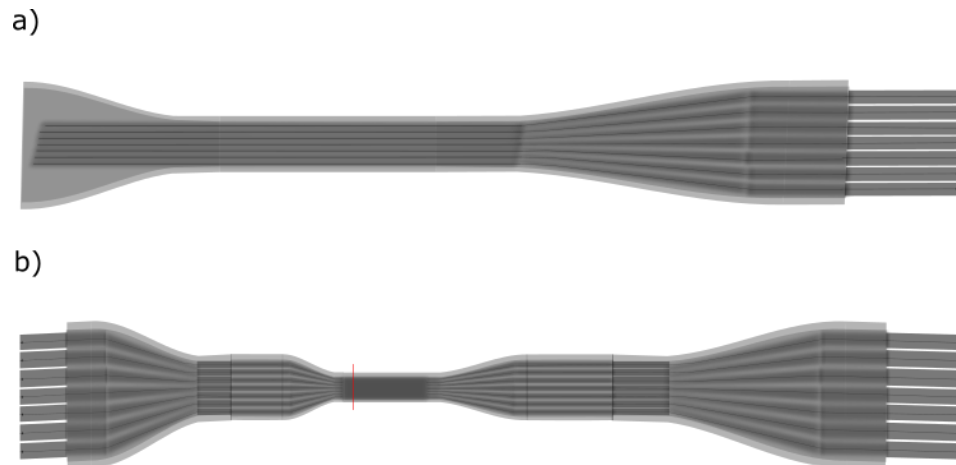


Figure 29 Tapering a) after the first one with the optical fibers without counting in the smallest section. b) The second one with a red line where it has to be cut.

The next step is to do the second tapering. To start, this process has more material than first tapering, that is why we had to use the Vytran with another chiller and a powerful filament. For this second tapering, putting the constant section of the Figure 29a in the filament. It will reach higher temperatures than those used for tapering. For cooling down the system, I used a chiller (coherent) normally used for cooling a laser system, which I adapted to be controlled from a computer

(annex). Once with the right equipment to do this specific tapering is ready, there are two parameters, the heat, and the velocity or tension. These parameters have to match to produce a uniformed melting.

As I was mentioned in the previous chapter, the fusion of the fiber is a critical aspect to have an adiabatic transition, low losses and a homogenous refractive index. For this last characteristic, the capillary tube has to cover and hold the optical fibers, like in a coupler for lasers [49], having less space in with air and an homogenous core of the PL.

Figure 30 shows the different steps to produce an optical lantern. The first one, the fiber is melted and pulled at a certain constant velocity to reduce its sizes, creating just tapering section consisting of a bundle of fibers. The second step is a semi-melting that happened increasing both the temperature and the velocity, having air holes in the last part. The final step is to produce a perfect melting. This is achieved by further increasing the temperature and the pulling velocity; this process is not linear. These images also represent transition of the fibers, starting with a bundle and continuing with the process of melting until their fusion.

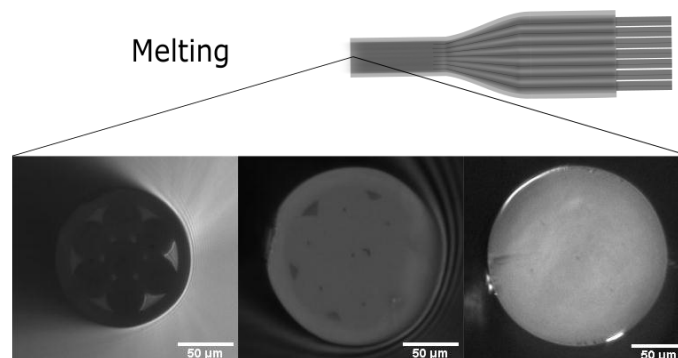


Figure 30 The transition of the melting. In the left, there is just a bundle of fibers. There is a semi-fusion of the fibers in the image of the middle. The last one is a complete fusion.

It is important to ensure that there is no space or air in the new core; because it will change the refractive index and it will generate some losses in the entrance

light. In addition, the velocity and heat will change depending on the material of the elements or on the number of fibers.

Some of the examples when things went wrong are shown in Figure 31. There, the velocity and heat affected the device was not the correct. Figure 31a shows a device with more power than the reduction one, but with the same velocity. It shows that the device moved slowly, giving a low tension, heating more and deforming it. Figure 31c shows a device using more power and high velocity, giving as a result, a fusion but with a not homogenous refractive index, due to, the air inside the capillary could not escape, deforming the melting of the optical fibers. Other cases are when the velocity was so slow that the PL, it was melted until broke itself or with a higher velocity that increases the tension until broke it.

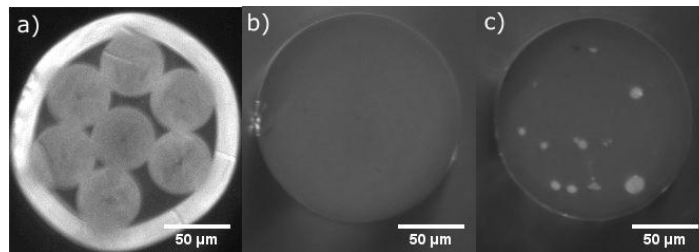


Figure 31 Tapering of PLs. a) More power than the reduction of the fibers and low velocity. b) Correct transition. c) High velocity and high power.

The melting is the principal generator of losses in the device, but this is not the only one, there are more kind of sources of losses, before the melting and after it. One problem is that it cannot be known if the process was right or not until the cutting part.

The last part is the cutting. Figure 29b shows the device after the second tapering and it has a red line, which is the right place to cut it to have the PL. This is there because the multimode section has to be enough length to work with it, also to do not have problems if you have to recut the device. The cut has to be precise, like in general in optical fibers, but in the lab there was no cutting machine with the

characteristics to perform the process correctly with the second tapering. So, an idea is to hold both sides of the tapered fiber when it is in the state of the Figure 29b and apply a force pulling them. When the tension is enough, you can do a line with a diamond pen, just to do a mark. After, the tension of one side has to increase until braking it. It will break, having the results like the images above.

There are cases When a cutting problem arrives, the results can be as shown in Figure 32a. In these cases, the front view will be like Figure 32b. Providing a problem in terms of losses, the light cannot enter in the right place, having reflections and giving less power in the output.

Another issue that appear after the cutting are like Figure 32c, in which one of the fibers was not inside the tapering section, generating a wrong melting because it does not have the right material, also the fiber do not fit with the capillary tube, generating two kind of losses.. That is why the optical fibers without coating has to through the entire tapering like in Figure 29a.

Another source of problems during the tapering process is when, in some cases, ethanol, dust or material were inside the capillary tube, giving as a result, Figure 32d. These situations produce losses due to the absorption of light for the material, the bad melting and the obstruction in the entrance. In the particular case of the ethanol, it can produce burnt parts, which will be black. To minimize this kind of issues, the cleaning part will have to be exhaustive and checking that the ethanol is completely evaporated.

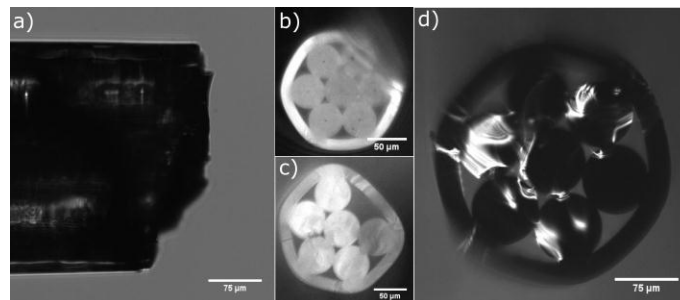


Figure 32 Sources of losses. a) A bad cut of the PL. b) Front view of a bad cut. c) Reduction of the fiber with just six elements. d) Dust or residual material in the PL.

In the annex, the building protocol is explained in further detail. This part explains the used machines and the parameters are specified.

Photonic Lanterns with an extended source.

The characterization of the PL with an extended source is the principal objective of this section, to see the advantages to do LS in the last chapter. For example, as mention in the previews chapter, a characteristic of a LED is the huge number of modes. Here it is possible to create a PL that can keep a high number of modes in the entrance. Thus, we will have more power than the usual in which an optical fiber or a bundle of fibers are used However, there is a problem, if we put a high number of modes, we will have to produce the PL also with more single mode optical fibers. However, it exists the possibility to use fibers not completely single mode (for example, sustaining several modes). Thus, we can create different PLs like in Figure 33, which have different sizes to hold some modes in the output to have more energy per single fiber.

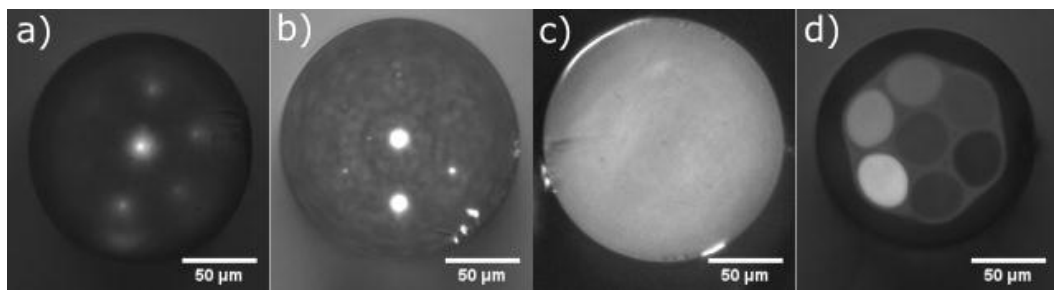


Figure 33 Photonic Lanterns made it with different kind of optical fibers a) SM450 ~ 3.4um core, b) SM800 ~5.6 core, c) SFM28 ~8um core and d) AFS105 ~105um core

Considering this, the light of the output will change depending on the number of modes, because the density distribution of light changes depending on the superposition of modes, leaving every PL for different tasks, like less power but with a smaller output beams of otherwise more power with larger output size. For all those cases, I performed some calculations in Excel to see how many modes can be inside of each optical fiber; changing their core diameter, the wavelength,

and their material (Table 2). In order to validate these calculations, I did a comparison between them and a simulation using a software from the University of Barcelona [50], to be sure and to have an idea of the different modes that travel inside the optical fiber.

Wavelength	Diameter	Delta refractive Index	Core index	V Parameter	Modes
600nm	4.7um	0.001	1.46	1.33	0.71691
500nm	4.7um	0.001	1.46	1.59	1.0246
450nm	4.7um	0.001	1.46	1.77	1.26972
600nm	9.4um	0.001	1.46	2.66	2.86763
500nm	9.4um	0.001	1.46	3.19	4.12422
450nm	9.4um	0.001	1.46	3.54	5.07887
600nm	18.8um	0.001	1.46	5.31	11.4274
500nm	18.8um	0.001	1.46	6.37	16.4452
450nm	18.8um	0.001	1.46	7.08	20.3155
530nm	8um	0.004	1.44	5.19	10.9168

Table 2 The number of modes of each optical fiber with three different wavelengths, changing the diameter and the required values to calculate the number of modes. Some values took it from a commercial enterprise.

To observe the number of modes generated experimentally, we have to introduce the light inside the PL, but this process have mainly three sources of losses. These sources are: the size of the image of the source (i.e. LED) in the entrance of the PL compared with its diameter, the divergence of the source and the NA of the image compared to the NA of the PL.

The principal task is to collect all the light and focusing it to have the smallest image with a low NA. In the case, I used a LED from ThorLabs. The best way to have enough power in the output of the PL was using the lenses included with the illuminator that can collect all the possible light and collimating it. Then, using a MO of 10X, the light has been focused to obtain a small image with NA with a size XX times larger than the PL (Figure 34). This was the best way because collimate the light was an easy task with their lenses. With the collimated light, the focused images can be smaller, giving as a result a small image with almost all the energy from the LED.

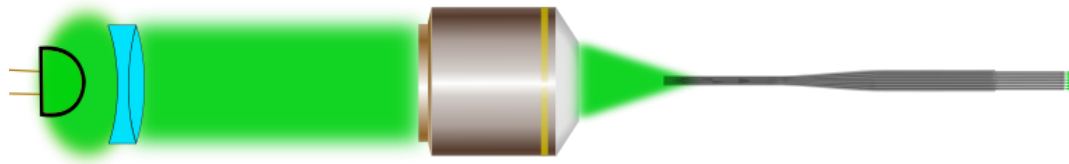


Figure 34 The optical path of the LED light for the optical system.

The possibility to use a different LED for a more powerful one was evaluated, but with a flat interface. This however, did not work properly as the divergence of the device was excessive. This is an example of why every LED will have to have its own assembly. In the case of such flat LED, two big lenses could be used to collect the entire light and to focus it with the most efficient collection of light while keeping low NA.

In any case, once you manage to couple light into the fibre, the output will have a profile that will determine the light that you can put in the PL. I used this profile to see where there are more losses in each case. For example, in Figure 35 the blue graph shows the profile of the focused beam, it is not homogenous because the LED is square and it is not continuous. Following the Foucault knife-edge test [51], I measured the power with a photodiode while the knife-edge is moving through the beam. With that, I could measure the real size of the focused beam by taking the FWHM of the derivative of the graph. In addition, I was able to calculate the NA using Pythagoras's theorem of two distances of the image.

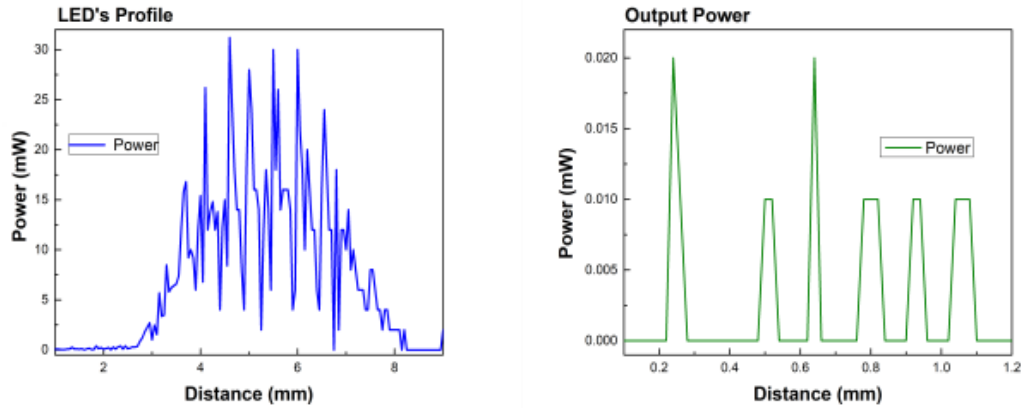


Figure 35 The blue graph shows the profile of the input light in the PL and the green one shows the output light of the PL.

As it is shown in Figure 35, the green graph shows the output of the PL, as it can be seen, there are still some issues. First, one fiber has no output. Second, four fibers have less power, whereas two are very efficient, showing two big picks. This means that there is room for improvements. In this case, the problem could come from the cutting step, damaging the fiber or from a problem in adiabatic transition.

In addition, having this profile of the output, you can prove how many modes are traveling inside the PL by looking to its front face, as shown in Figure 36. Here Figure 36a shows the behavior of the different fibers, its profile and that each output has a different focused plane. More importantly, Figure 36b shows that effectively there is superposition of the modes, the two zooms show the profile of the output. Both images are from the same PL but the first one with 530nm and the other one is with a 780nm. On the other hand, it shows that the cores are not in a line, also that there is more power in ones than others and they have a different focused plane.

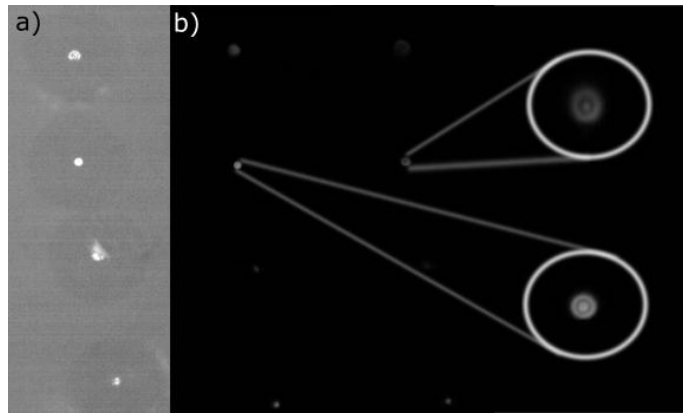


Figure 36 Pictures of the output light a) Front side of the PL. b) Two images of the front side using different wavelengths. The first amplification is with around eleven modes considering a green led with the peak in 530nm that it showed in table 2. The second amplification is with a peak in 780nm having around six modes.

Comparison of an optical fiber and a Photonic Lantern.

In this section, I am going to compare the transmission efficiency between a PL and a bundle of fibers. In order to do so, I will compare the PL with a single optical fiber and estimate the effect of having multiple fibers.

In order to perform the first preliminary test, the fibers used in this project were the most common optical fibers from telecommunications. These fibers are single mode fiber for 1550nm (SMF 28). The cladding's diameter is 125um with a core of 8um of diameter.

On the other hand, using seven SMF28 fibers, after the tapering, the PL had a diameter of 175um in the multimode section.

To consider the effective area for the comparison, it is necessary to know the sizes of the profile of the focused light of the LED, which had an area of 0.08675mm^2 with 2.16mW of power, to calculate the energy density. Then, calculating the energy density of the focused part of the LED we can estimate the power in the entrance of the PL and obtain an approximation of the output power, in an ideal behavior (Table 3). Dividing the experimental power between the theoretical power

in the specific area, it has losses of a hundred times. Both have almost the same sizes, but the comparison was in the density of energy.

The PL collected more power than the optical fiber giving a factor of 4 times more. This result was done considering the LED's profile of Figure 34 of this chapter. In that case, the optical fibers of the PL were not optimal. In the bet of the cases, the PL, the factor can increase to 6.6, this is just an estimation. On the other hand, this is just for seven optical fibers, increasing the number of fibers, the factor will increase due to, energy conservation, and using better materials the system could also improve.

	Area	Theoretical Power	Experimental Power	Power EP/TP	Power out/in
SMF 28	0.012mm ²	30.55 μW	0.02 μW	0.00065	
Photonic Lantern	0.022 mm ²	56.51 μW	0.15 μW	0.0026	4.05
Photonic Lantern Best cases	0.022 mm ²	56.51 μW	0.245 μW	0.0043	6.62

Table 3 Characteristics of the SMF 28 and the PL with a LED of 0.08675mm² of area and 2.16mW of power. The last results are optimizing this PL in the output.

This is proof that the PL has a better response to carry more power than a fiber or a bundle of fibers, for the size of the bundle of fibers; it is possible to create a bundle of PLs to have more power in the output from the same size.

Another comparison is just considering the effective area of the core, in the optical fiber, the 8um core gives an area of 5.026×10^{-5} , giving the power of 0.125 μW and experimentally is 0.02.

In the case of the PL, The area of the cores of 2.66 μW each one that multiplied for 7 gives 3.907×10^{-5} , having 0.097 μW of theoretical power and experimentally it gives 0.15 μW , giving more power due to the decoupling of modes for the complete fusion of the PL. If there is a bundle with the same sizes as the multimode section of the PL, it will have less power than the PL due to the space with air, where light will stop or will travel outside of the device.


Chapter 5: Light sheet with photonic lanterns

In this chapter, I am going to implement the Photonic Lantern to a Light Sheet Fluorescence Microscope to produce 3D fluorescence images. I will determine the thickness of the obtained Light Sheet (LS) and the characteristics of the resulting Light Sheet device. Besides, I am going to explain the results showing images of *in vitro* samples.

Usage of PL in LS

The behavior of the PL shows that is possible to create a LS with the necessary characteristic to do high resolution with LSFM and this is considering a PL with not the best parameter and materials. Maybe the losses could be several but to work with alive samples, the irradiation has to be low. Considering this, the PL collects all the light possible, giving in the output, enough power to do fluorescence to do LS. The PL produces spatial coherence and removes the image of the LED creating point sources.

The construction of this PL gives all the characteristics to have a LS compared with the experiments presented in the chapter of sources of light. Here there is more power to create LS, there are several point sources with spatial coherence and few modes to create a LS with a small thickness.

To use a PL in a LSFM, the setup will be like  Figure 37. We will use a basic LS system from the cylindrical lens to the camera but we will replace the laser and collimator by the PL.

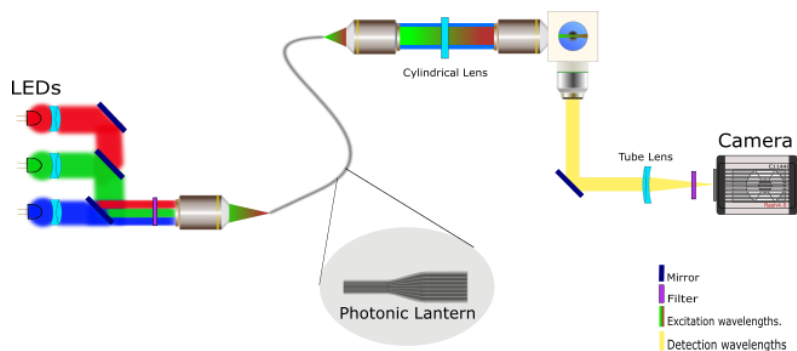


Figure 37 LSFM with a PL for different wavelengths

The LSFM system is very sensitive to any light as fluorescence is usually very faint. On the other hand, the high divergence of the LED as seen before, introduced the difficulty to collect all the divergent rays. The non-collected light is then emitted in all directions and can interfere with the LSFM. Because of that, I placed two boxes, one in the illumination part from the LED to the first part of the PL to isolate this part. The second one has been placed around the camera to remove all the light not coming from the optical path. This second box is critical because the cameras are so sensitive to detect since a single photon and the parasitic light can appear everywhere. As the filters are placed at a certain distance from the detector it could detect all the wavelengths.

An essential point is the MO or the lens to collimate the coming light. This lens must have the same NA as the PL to reduce losses. Also, to have better images of fluorescence, it is important to put a spectral filter just after the LED to provide only the right band for fluorescence excitation. In fact, due to its large bandwidth, the LED excitation light can reach the bandwidth of the emission filter.

Once with this system, there will be three more issues in the generation of LS caused by the PL the focusing, the alignment of the fibers in position and light traveling inside the cladding. To look at them, it is necessary to use a mirror in the mounting part to watch the output of the PL with the cylindrical lens. Figure 38a shows the problem of focusing, the fibers are not placed in the same plane for some micrometers. The second issue involved is that this is a handmade system,

and one of the problems was placing the optical fibers in the right position to avoid errors. Each optical fiber will have its own focal plane, but this could be solved by using a machine to have a better precision.

Figure 38b shows that there will be several light sheets and putting all together, the result will be the LS in Figure 38c. The LS will be a superposition of light sheets. Something important here, it is that there are a large bandwidth and no temporal coherence, giving a uniform LS without interference. On the other hand, there are some inconveniences with the PL, the length is not enough to absorb the light inside the cladding, giving a LS with a halo, which is the third issue. This problem corresponds to the creation of the device, using optical fibers with a bigger length than 50cm, it could be solved. Furthermore, the LS is not in the right position, it is in a horizontal plane and it will have to be in a vertical plane to have the camera in the same position as in the setup before.

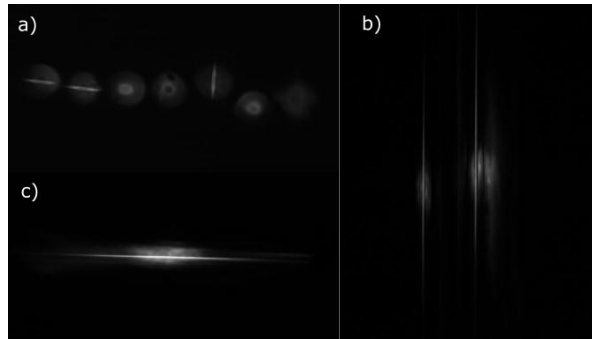


Figure 38 Front view of the optical fibers. a) Seeing the focused plane and with magnification, b) CL with the axis in the horizontal plane, with respect to the table. c) CL in a vertical plane with respect to the table. In all the cases the light travels inside the cladding too

Thus, there will be four different possible positions between the PL and the CL. In two cases there will be several light sheets and the second one the superposition of every LS will give just one. There are two possible configurations, each one with two combinations horizontal and vertical. This happened due to the CL collimate in one axis and focused on the other one, as mentions in the LFSM chapter. In Figure 38b the collimating part is the vertical axis and the horizontal one is the

focusing part. In Figure 38c the collimated part is the horizontal one, so, focusing the LS.

The solution of those problems is respectively; to collocate the optical fibers in the same distance to the collimated MO for the focused plane to create a longer PL to filtrate the light and to place the PL in a rotating mount to have all the LSs in the same axis.

Solving these, the focused plane will be almost in the same plane as in Figure 39a, that it was seeing it without CL. The noise produced by the light in the cladding is removed for the absorption of the optical fiber and the rotation of the new mounting of the PL allows having better control of the LS (Figure 39b and Figure 39c) and the CL to have a vertical LS. More details about the alignment of this part are detailed in the appendix.

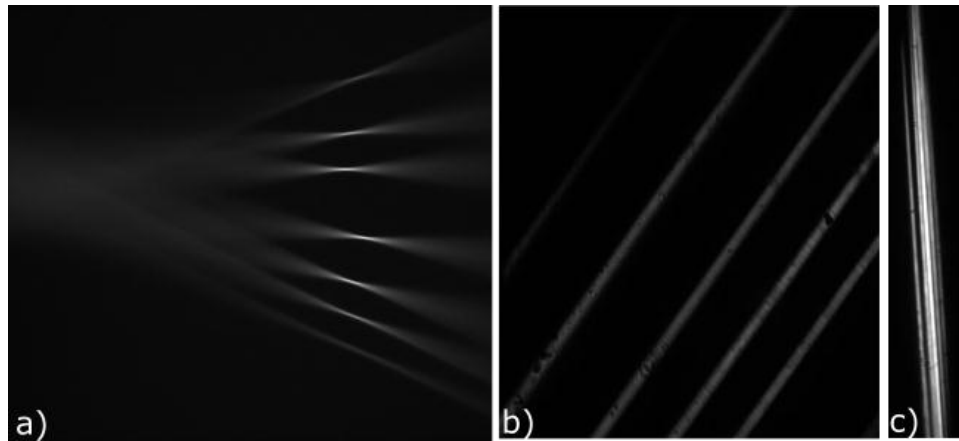


Figure 39 Characteristics of the new mounting. a) Lateral view of the focusing, b) and c) front view rotating the PL.

In conclusion, considering that the light has been focused on a line, it has been possible to create LS with a superposition of point sources with large bandwidth. This demonstrates that it is possible to do LS with a LED.

Characteristics of the LS in PL

In the previous section, it has been shown that the LS is created by the superposition of several individual LS from each of the single mode fibers. The relative orientation of the aligns fibers and the cylindrical lens is set by rotating one respect to the other. In the ideal case, the thickness a LS produced by a single fiber will be the same as the superposition of all. However, as it has been mentioned in the previous section, if the optical fibers are not aligned for some micrometer and they are not cut perfectly the result can be not as the ideal introducing an enlargement of the thickness of the LS. To corroborate it, I measured the thickness of every LS and the superposition of them, in both cases using a MO of 10 to collimate and to focus. Here appear the problems before mentioned; the focused plane is different for each one. Figure 40 shows 4 images of 4 LSs, each one represents a different focused plane of each LS, giving 6.169, 7.32, 4.47 and 4.12 of thickness for each LS. Thus, the minimum LS has to be around 7.5um, but doing it, the thickness gave approximately 8um, this happened because when it is focused, the other LSs will not be in the right plane, producing a halo and increasing the thickness.

These issues can be solved by the alignment of the fibers and a better repositioning. It can be also improved by polishing the output. However, it is worth to notice that this is the LS with the lowest thickness with an incoherent source than having never been reported. However, it can be still improved to have even smaller values.

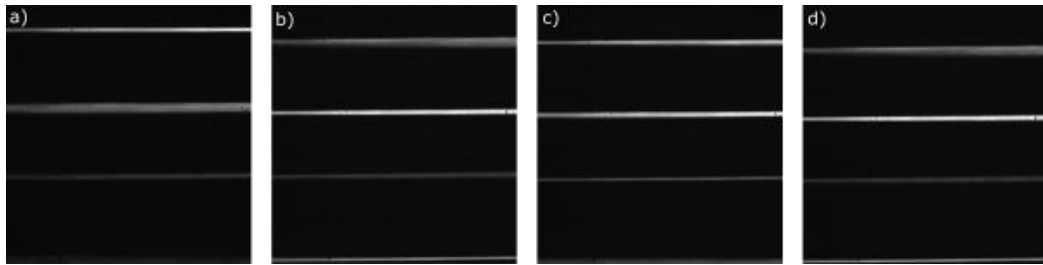


Figure 40 The light sheet of the PL, in each image the focused plane was for a different line. a) Focused for the first one with a thickness of 6.169, b) the second one with 7.32 of thickness, c) 4.47 and d) 4.12.

To emphasize the last idea, in the previous chapter, the last result of Table 2 shows the number of modes with a green LED, which was used to do these results and has several modes. Working with a fiber with 4.5 μm of core diameter that is the single mode for that wavelength, it would give smaller LS. In the opposite case, increasing the core's diameter, it would have more power. The possibilities increase and the applications for each one too.

Comparison with standard LSFM

In this section, we will introduce a laser to the system, keeping the new illumination method. Using this setup, we will capture images in the following modalities and then will be compared with the laser modality. The setup was like Figure 41.

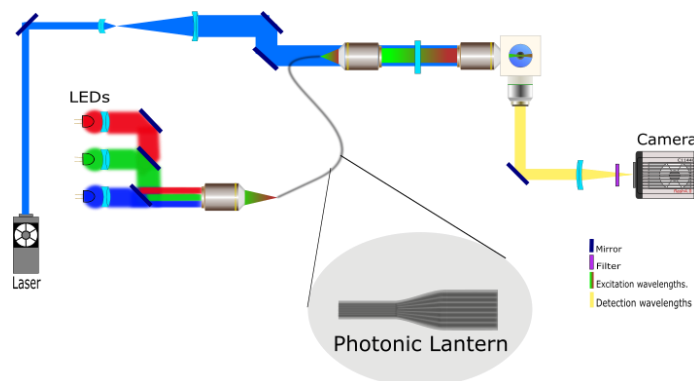


Figure 41 Light Sheet Fluorescence Microscope with both illumination systems

The very first images that demonstrated the functionality with the homogenous LS were from a zebrafish egg. Figure 42 shows the comparison between the LSFM with a laser and an incoherent light. Figure 42a shows three steps, the first image was with wide field, the second one is an image of a stack of the sample with a laser LS around 2 μ m, the last one is the maximum projection of the stack.

In Figure 42b there are four steps, the first one is the bright field, the second one is two images one corresponding with scattering and the other with fluorescence using the PL. In this case, the LS had a thickness around 8 μ m with less 0.15 μ W of power after the MO, the last one is the maximum projection of the stack of scattering. There is not a maximum projection of fluorescence stack due to the low signal to noise ratio.

The limitations in this set up were the power of the LED, the position of the LS and the thickness of the LS that is larger compared with normal ones. That is why the images in fluorescence have a very little signal. In the case of scattering imaging the LS was not powerful enough and for the bad alignment of the fibers gave a LS a little bit rotated. To have in the right position the PL with the CL, in appendix it is explained how to get the best LS.

All the samples were mounted in agarose with a capillary tube to have the same refractive index.

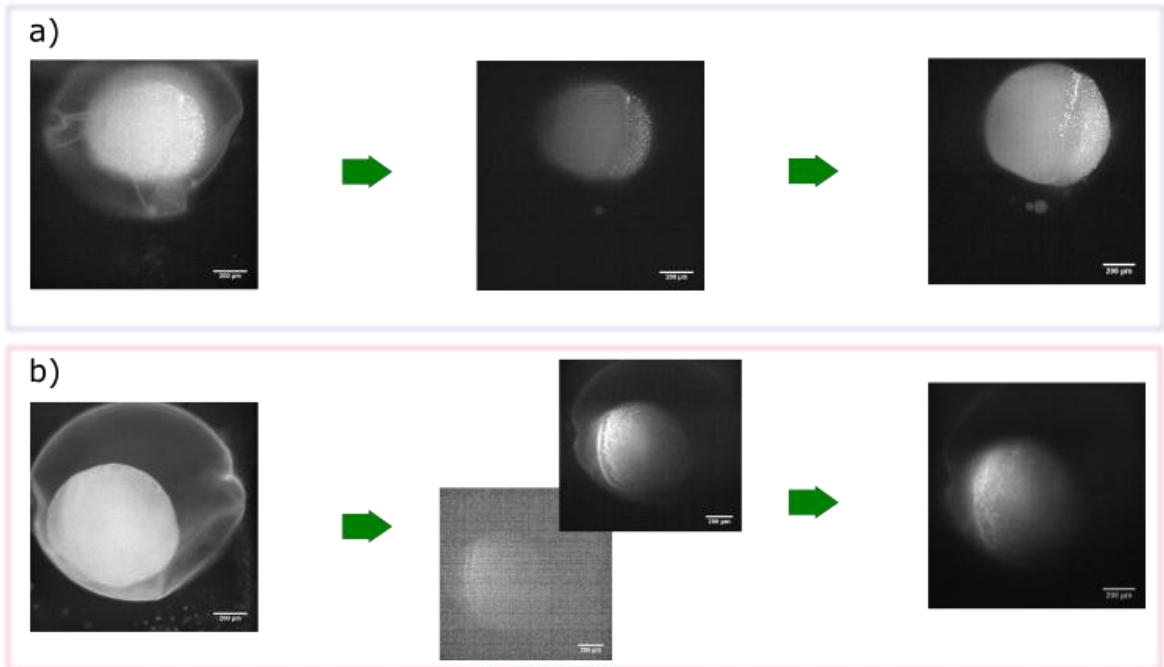


Figure 42 Images of a zebrafish egg, a) the first section is composed by the image of bright field, a section did it with fluorescence with the Laser and the maximum projection of the stack. In the other case, b) it is the same sequence, just adding the scattering imaging and in the last image removing the maximum projection of fluorescence, with was more noise than image.

Changing the MO from 10X to 20X provided a thickness of the LS of around 5 μ m. Changing the thickness, the density of energy changes too, having more light in the focused area. This thickness is approximately the same to a normal one using a laser, but again, this LS is with around 10 modes in the output of each fiber, it would be smaller, using mono mode fiber.

Changing the sample for spheroids that are standard in microscopy. Figure 43a shows the maximum projection of the spheroid acquired with a laser with a LS of 2 μ m. Figure 43b shows the images acquired with scattering using the PL. Here there is still a problem, which is the power. It was not enough to do fluorescence, also because the samples are old having low labeling. New fresh samples are required to get nice fluorescence imaging.

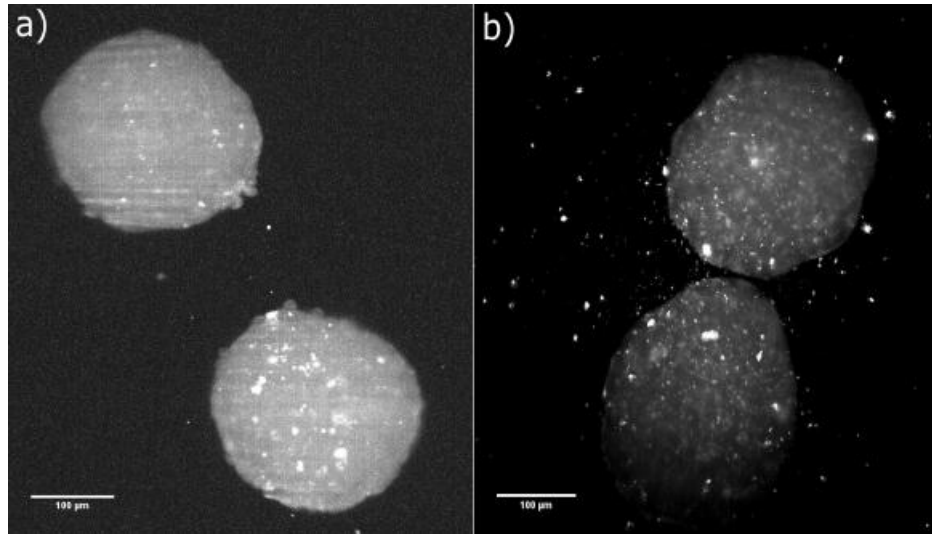


Figure 43 Cancer Spheroids, a) Fluorescence image did it with laser b) scattering image did with a LED and the PL

Figure 43b is the first scattering imaging with a LED reported in Light Sheet Microscope.

Next results are using zebrafish embryos due to the easy provision with the required labeling. The embryos were selected with 48h after birth because there are more visible structures with scattering and it is easy to work in the tail to remove the auto-fluorescence of the yolk. The yolk is the part of the fish that is fed in the first days. Also, the yolk produces aberrations for its spherical shape and different refractive index, acting as a lens.

Another change was the LED for other ones with more power. The images obtained are shown in Figure 44. These show the maximum projection of each stack in an exposition of time of 100ms and 1 of binning. The Figure 44a, Figure 44c, and Figure 44d were done with the PL generating a LS of 5 μm of thickness. In the case of the Laser (Figure 44b), the LS had a thickness of 2 μm .

The first and second image are of fluorescence, the third one has fluorescence and scattering, with just one filter, and the fourth one is imaging scattering. This is why Figure 44c and Figure 44d are very alike, and only the second image is from a different part of the tail of the zebrafish.

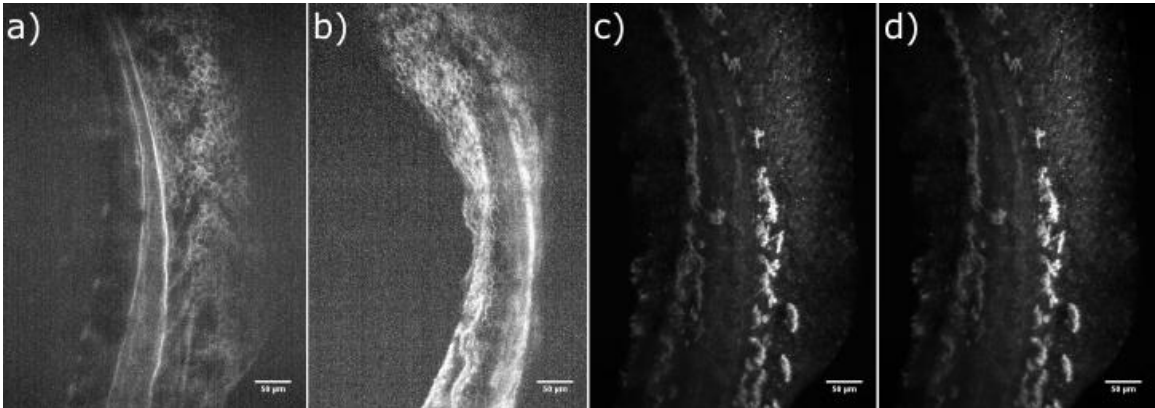


Figure 44 Images of fish tail, a) with the PL producing fluorescence, b) fluorescence with the Laser, c) removing the filter of illumination to see fluorescence and scattering and d) removing all the filters.

The first three images have the same power in the input, approximately 1.25uW but with different density energy for the size of the thickness. The fourth one has less current from the battery because there are no filters in the illumination and detection part, it leaves more light to pass. Here the big bandwidth plays an important role to do scattering and to take advantage of the LEDs to use less power than the required to acquire fluorescence.

Figure 44a and Figure 44c have the same power in the illumination, with the same LS, the only difference is the detection filter. With these two images, the experiment rectifies that the scattering is more presented than fluorescence, in this kind of samples.

Next set of experiments were done with 1s of exposure to obtain a better Signal to Noise Ratio, the images look like in Figure 45. Figure 45a is the image did it with the laser and Figure 45b with the LED, in both are possible to see the structure of the cells.

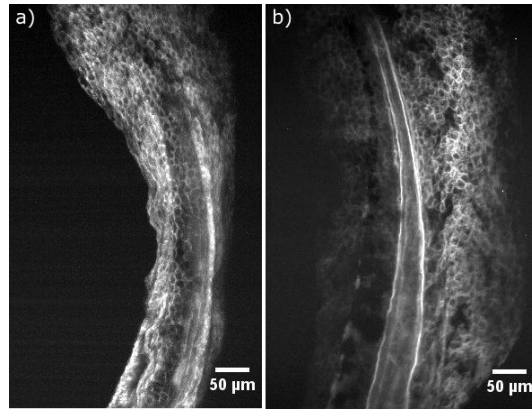


Figure 45 Zebrafish tail, a) image using a Laser and b)) image using a LED with the Photonic Lantern.

To have a better comparison, the setup was improved to have an easy way to change of illumination method, to see the same part of the tail. The last set up was Figure 46, where to change from the laser to the PL, there was a mirror that has in a flexible mounting.

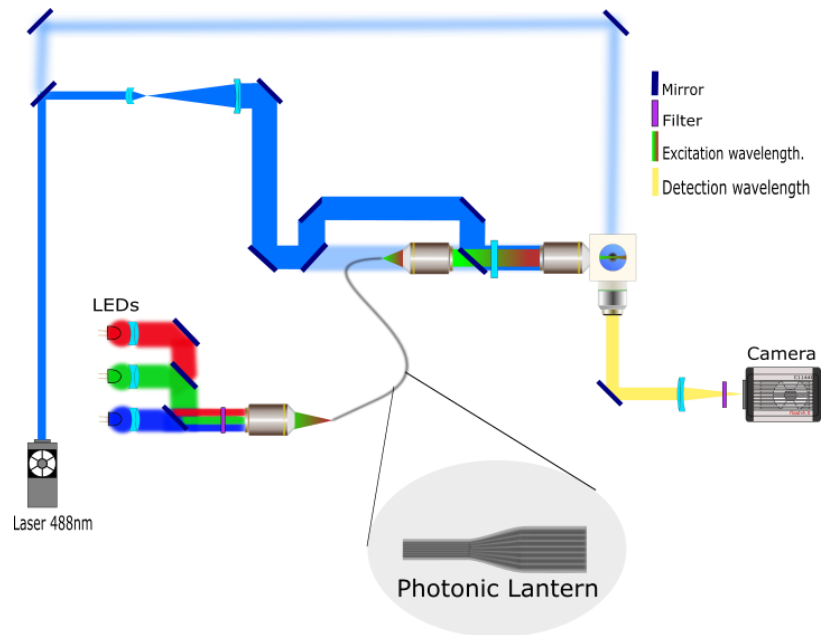


Figure 46 Setup with different optical paths, the blue one is of the laser to do images, the blue blur optical part is of the alignment, the three colors come from the LEDs and it passes through the PL, and the yellow one is the detection wavelength that will depend on the source of light and the kind of imaging

Having this setup, the resulting images are better to do a comparison of both illumination methods. The four images from Figure 47, show the same section of the tail but with different characteristics. The first two were done with 100ms of exposure time and 1 of binning. Figure 47a is an image of fluorescence with the laser and Figure 47b the illumination part was with the PL and the LED. Changing the exposure time for 1s, the images improve being Figure 47c with the laser and Figure 47d with the LED.

In those cases, the images with the incoherent light do not have so present the lines that have the images with the laser, this proves that the homogenous LS is improving illumination and the images. Furthermore, the images have enough resolution allowing the visualization of the membrane of the cells.

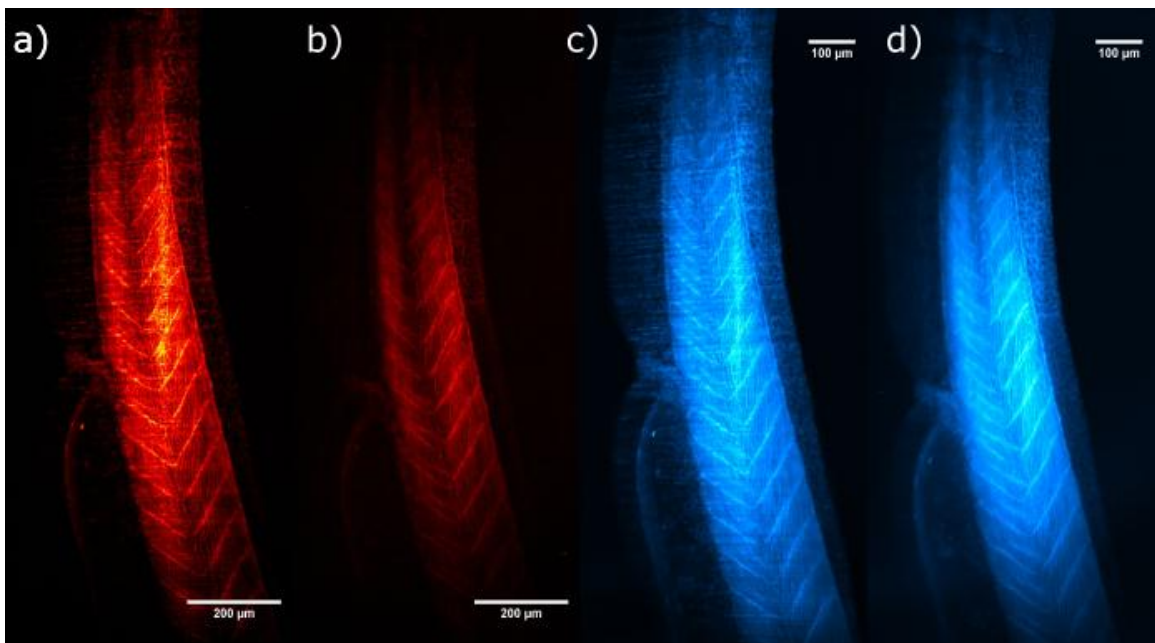


Figure 47 The red images represent the tail of the fish a time exposure of 100ms, a) image using a Laser and b) image using the PL with the LED, the blue images are with 1s of exposure time using c) the Laser and d) the PL with the LED.

The next table summarizes the comparison between the different generation modalities explored: Laser LS, LED LS and PL LS. As it can be seen, the LED with the PL generate a LS with the advantages of the other two, giving as a result, a

homogenous LS, with enough power, do not produce interference or speckle and with Low cost, which can improve.

Characteristics	LASER	LEDs	LED with PL
Interference	High Length Range	Low Length Range	Low Length Range
Speckle	Yes	No	No
Enough Power	Yes	No	Yes
Cost	High	Low	Low
Thickness of LS	1~5um	20um	~5um (could be less)
Bandwidth	Small	Big	Big
Modes	One	Several	Some

Table 4 Characteristics to do LS with a laser, LED and the novel illumination

Three color imaging and Scattering

Once the high resolution of the system has been demonstrated, the next step was to acquire four-channel images. This means three colors with fluorescence and the fourth one with scattering. To rectify that the acquisition of images are of fluorescence and not scattering, a wrong immunostaining helped to check that using two filters it is possible to see only fluorescence (Figure 48). With these images, the best result is presented with Figure 48a because it is produced with scattering, which does not require a labeling or a high power. The sample can be in a more natural environment than with labeling.

I prepared the samples to have the best labeling, the membrane with GFP in 488nm (Figure 48b), immunostaining with alexa 532nm in tubulin (Figure 48c) and staining with phalloidin 625nm in actin (Figure 48d). The protocol is described in the appendix.

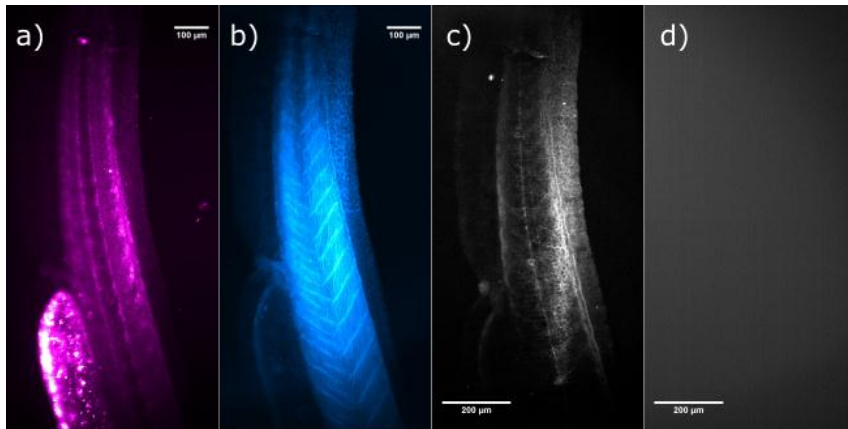


Figure 48 same section of the tail, a) scattering imaging, b) membrane, c) a low staining that with imaging processing can see something and d) nothing in the red channel. The illumination has a filter with different bandwidth of the detection to do not see interference, this image show that the filter works well and the staining no.

Changing the labeling for membrane with GFP in 488nm (Figure 49b), immunostaining with alexa 532nm in tubulin (Figure 49d) and another immunostaining with alexa 630nm in mitochondria (Figure 49c). A good label of the samples will be like Figure 49, which also shows imaging scattering (Figure 49a) and the superposition of all the color to make the tail of the fish with all its structures (Figure 49).

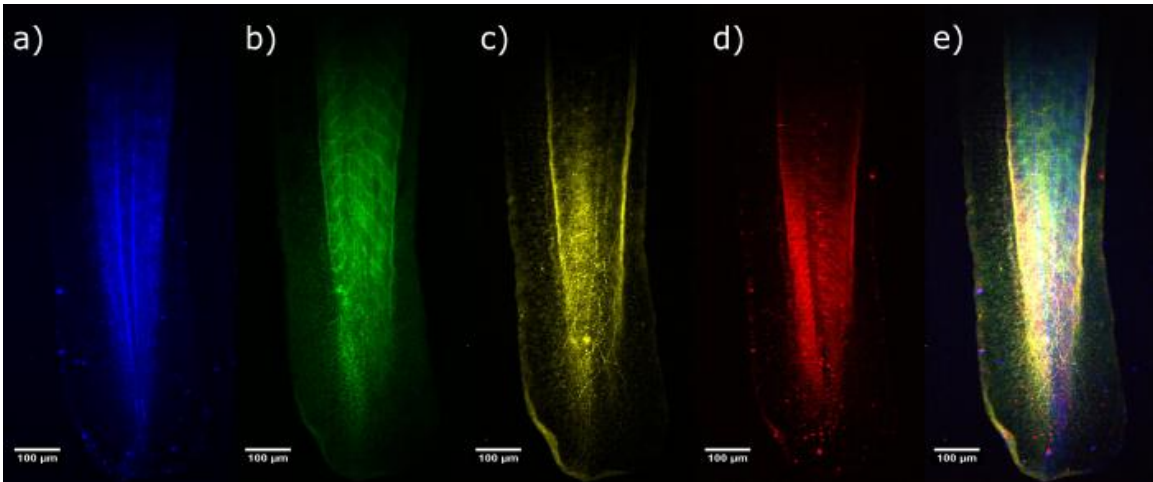


Figure 49 Images of the zebra fish tail, each image shows different structures, a) the one produced with scattering, b) membrane, c) tubulin, d) mitochondrion, e) the superposition of all the channels.

For the superposition of the samples, it is important to have the right alignment, this can be checked visualizing the cross section. Figure 50 shows a transversal section of the fish. In this sequence of images, I added a translation in the different channels to rectify the position of the colors.

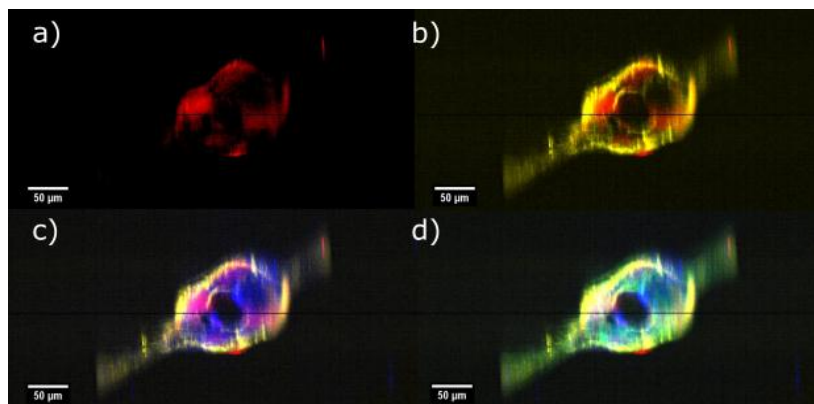


Figure 50 Cross section of a part of the Figure 49, since a to d there were added channels a) mitochondrion, b) tubulin, c) scattering and the last added was d) membrane.

The last example with four color is just to show the high resolution that this new device has. The labeling was the same as before. With the raw data and image processing, it is possible to do zoom in some sections of the sample like figure shows.

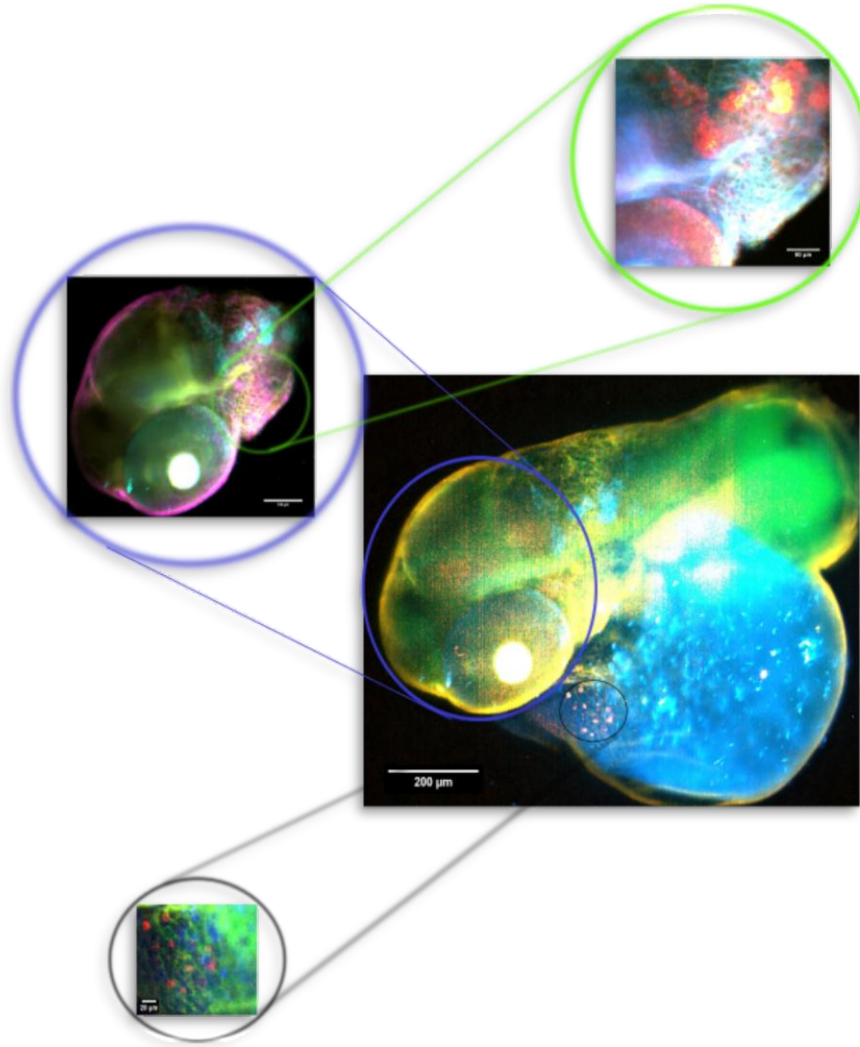


Figure 51 Image of a zebrafish with 48h hours with four different structures: membrane, tubulin, mitochondrion and scattering. The black circle shows a zoom of a specific section. The blue circle shows that it is possible to select just one part of the sample to have a zoom of the zones that it is not possible to see like the green circle. In the super position of the structures, the color are combine producing with parts.

On the other hand, using other samples without dyes, to observe the structure that can be done with scattering are Figure 52. Every plane of those images are like a dissection of that plane, because with the human eye observe the elastic scattering of the objects. These images are like an histological cut.

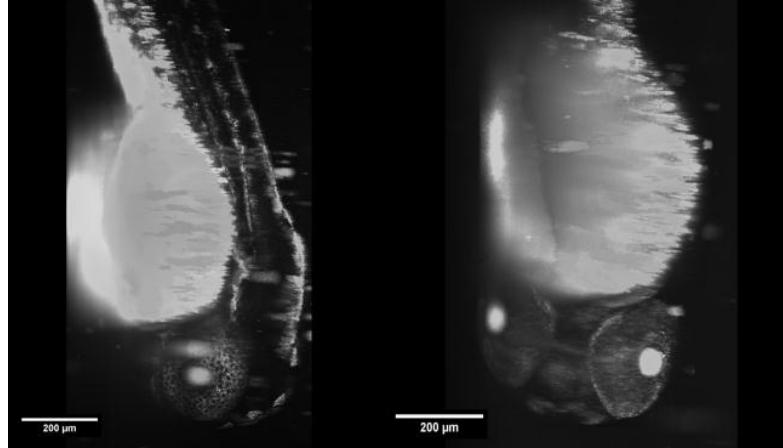


Figure 52 Images of zebrafish with 48h after birth, the left image show a maximum projection scanning since a lateral view, and the right image the scanning was since the head.

Chapter 6: Conclusions and future work

This thesis shows the first Homogenous Light sheet with incoherent light, improving the LSFM technique, using a PL and having high resolution. One part of this work was to understand and learn this technique to reproduce it in Mexico, which will be one of the future works.

Besides, the tables from this project shows the possible thickness of LS than can be generated with a laser, a LED or a LED with a PL, Showing its characteristics of each one. Also, the efficiency of the PL compares with a bundle of fibers. In addition, it is shown the important aspect or characteristics to create a PL proving that it is worthy for this specific application.

Using different PL, the illumination method will change depending on the number of modes of each fiber. Also, there are the first scattering images with a LED and the first images of fluorescence without a Laser. This kind of illumination will bring a new field of research, to produce more tools for microscopy or other areas.

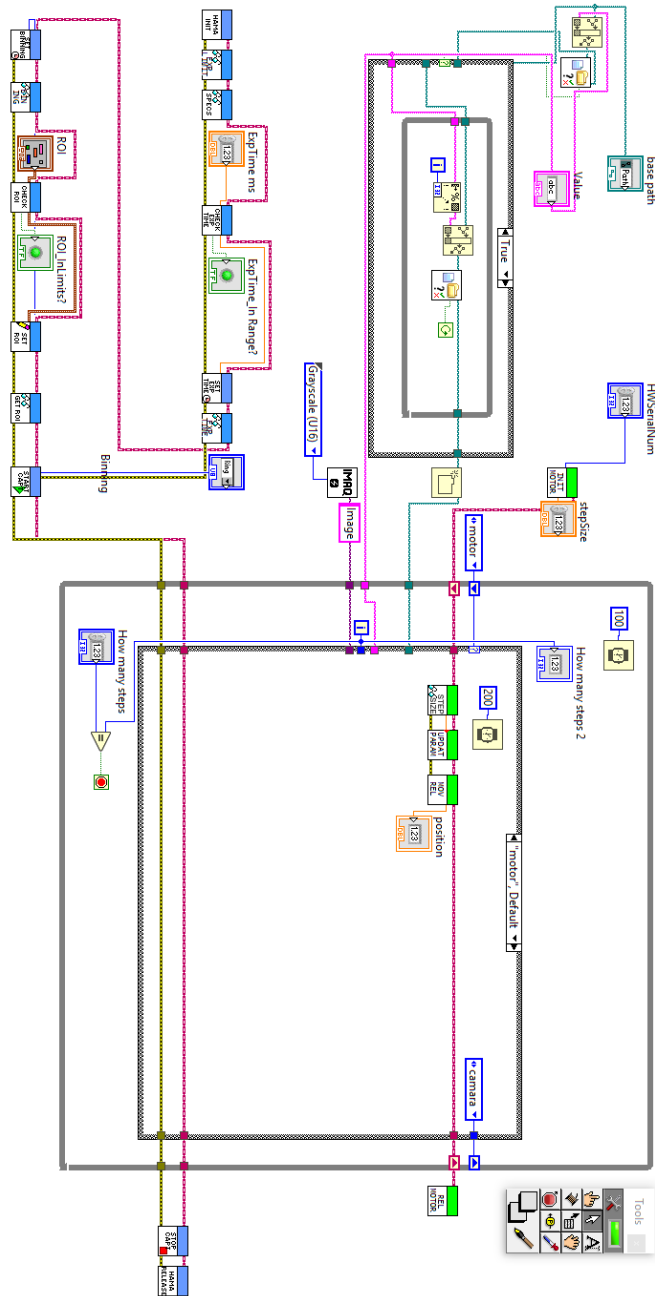
In terms of Intellectual property, the results of this project will provide at least one paper in an indexed journal, being the first author the author of this thesis.

There are several applications for this new device, for example, to see the movement of some cell without a perturbation (a dye). Observation of the sample in its natural environment.

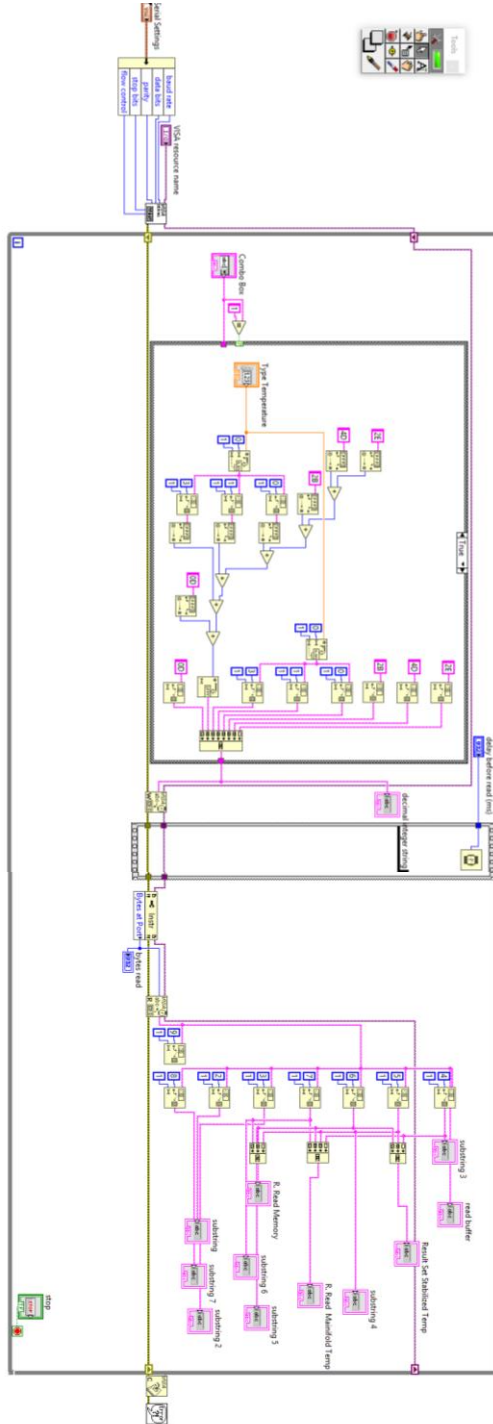
In the case of this project, several aspects can be improved on the engineering of the PL like the cutting of the tapering, the materials, find the smallest thickness of LS with this technique, placing in the same distance the optical fibers and more.

Appendix

Program to control the acquisition of images



Program to the chiller



In this part of the Appendix, I explain some important parts of the PL, I show some program that I did for this project and the datasheet of materials and machines.

This section consists of a technical way to create a Photonic Lantern and to implement it in a LSFM.

Making a Photonic Lantern

A brief review, to build a Photonic Lantern it is necessary to have optical fibers and a capillary tube and do two taperings.

In case of the optical fibers, you have to consider their cores because the size of the last light sheet will depend in the number of modes as I mentioned in the thesis. That is why, having a respective number of modes the light sheet will change in thickness. An example was with a SMF-28 (optical fiber single mode) that has $8\mu\text{m}$ of core; with this, it is possible to generate a LS around $8\mu\text{m}$ with and MO of 10X or a LS around $4\mu\text{m}$ with a MO of 20X. In addition, when there are modes that produces a dark ring like figure 1'a from figure 38. The modes will produce more than one LS with just one fiber, the LS will produce something like figure1'b, in a rough way. Remember that in table 1 you can have an approximation of the number of modes to have more power with a large thinness of a LS or less power but with small thickness of the LS.

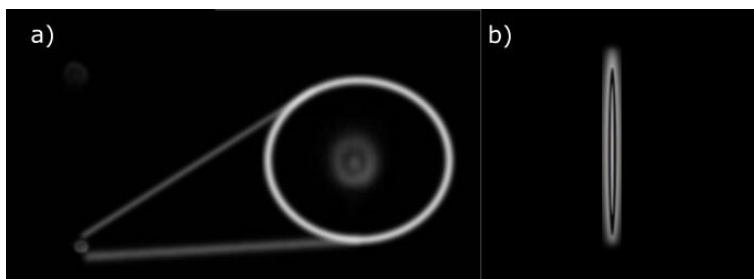


Figure 1' a) Modes in the output of the optical fiber b) this mode with a cylindrical lens

With the right optical fibers, the next step is to buy the capillary tube that must have two characteristics, the first one is lower index refraction than the cladding of the optical fibers to generate a waveguide. The second one, the inside diameter has to be bigger than all the fiber together, to put all the fibers and enough material in the outside diameter to hold all the process. With that, you can have an approximation of the multimode in the entrance.

In my case, the capillary tube that kept those characteristics were so expensive. Fortunately, just to prove the concept, the idea was to buy a capillary tube of fused silica to hold the fibers and do not have problems with the high temperature of the tapering. The capillary tube was Capillaries F300. Length = 20cm +/- 1cm from Photonics Bretagne with code C810-1020-SIL.

The next step is to do the tapering. For that, I use the GPX3400 - Vytran Automated Glass Processor Workstation from THORLABS, which had tools to work just with optical fibers and not the sizes of the capillary tube. To solve this problem, first the changing of the chiller was necessary for one used in lasers (brand coherent) that control low temperatures, but the display was not working, to control it since the computer, I did a LabVIEW program. Another essential tool was the Graphite Filament Assembly FTAT4 from ThorLabs to work with the sizes of the capillary tube (inside diameter 800um and outside diameter of 1000um) and with all the material by optical fiber and the capillary tube.

Before to use the machines, remembering the two tapers has to be to keep the decoupling of modes it is important to do the adiabatic transition in the second one. In the literature, there are few papers with the distances of the fusing, but there are no papers with the velocity and tension. Also, this PL will require different aspects. For example, the number of modes and energy. If there are a lot of modes or a big area to introduce more light, it is possible to create a LS with enough power. The decoupling of modes in this application is to have enough light if we have a perfect decoupling of modes but in a tiny area, we cannot introduce enough light in the system. Another point of view is if there are few modes (from a LED) or small size of the irradiated area, the power will be less, by the other hand, if we have a big

area and many modes, the decoupling will not work. The perfect transition for this application is between them.

Some references are cited in the thesis or you can find it in [56]. There, to do a Photonic Lantern of 7 fibers they use 4 cm for the transition section with the multimode section, obtaining a Photonic Lantern of around 110um of diameter. In our case, the size was 1.5cm in the tapering section and 1 cm in multimode section, giving 2.5cm of this complete section with around 175um of diameter.

The main goal was to start to understand this device, check if there were vantages against a bundle and to start to have a homogenous core. The showed Photonic Lantern in this thesis was not optimized and it is not the best one, it can improve.

Having this length, the next step is to start the first tapering, but for that, it is necessary to have capacitation from ThorLabs or the team manager, to know the properties, programs and characteristics of the GPX3400 – Vytran.

In a breve way,

1. Change the Graphite Filament
2. Change the holders for your capillary tube size
3. Turn on the machines.
 - a. This involves every part of the machine, Chiller , Vytran...
4. Select home/zero for all the system that involves every motor
5. Select the program
 - a. For this first tapering, it was selected a normal tapering with its characteristics in the program. In this case, the transition was 2:1 to decrease the capillary tube to the half because for this first tapering the principal function was to hold the optical fibers without coating. That transition was in 30 mm and having the smallest size constantly in 20 mm. This part will depend on how many fibers you want to put, also the density, sizes, and material of the capillary tube and its inside diameter. For the mentioned characteristics of the capillary

tube, the best power to do (in term of temperature) was 145W with the velocity and the characteristics of the common system.

6. Align the system to put the capillary tube in the middle of the filament.
 - a. This is in the three axes (X,Y,Z) and here you will need two capillary tubes to align one mounting to the other one.
7. Remove the capillary tubes
8. Select the command to maintain the filament up after the process
9. Move the right motor two small steps
10. Select anti back slaws
11. Start the process without the capillary tube.
 - a. To eliminate dust in the filament, check the distances of the motors.
In this case, you do not have to put the 145W, it can be 90W or less
12. Select the option to start a new tapering
13. Clean the capillary tube
14. Mount the capillary tube
15. Move the right motor two small steps
16. Select anti back slaws
17. Check the characteristics of this tapering (145W in this case)
18. Start the process
19. Remove the capillary tube

Having the tapering, we have to introduce the optical fibers there. To do it, the preparation of the optical fibers is the next:

- Cut the number of optical fibers
 - In this case was 7 and the length has to be more than 60cm
- Clean the optical fibers
- Remove the coating of a section
 - This length has to be bigger than the tapering section; in this case, I remove 40mm
- Clean this section
- Put together the fibers

- Every end without coating has to be in the position to cut the last part of the fibers to have the same lengths and to introduce everyone together.
- Wet the fibers with the liquid to clean it
 - This is to use the capillary force of the liquid to keep together the fibers
- Insert the fibers in the capillary tube Figure 2'
- Inject air to dry the liquid or wait with heat in the device.

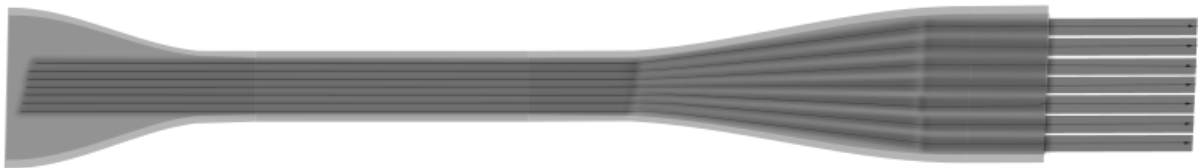


Figure 2' After first tapering with the optical fibers inside.

Clean this device, dry it and put together all the fiber are very important to do not have bad results like the mentioned in the thesis. After that, the next step is to do the second tapering. If you turn off the computer, all the protocol have to be repeated, if not you can jump the aligning part.

1. Change the Graphite Filament
2. Change the holders for your capillary tube size
3. Turn on the machines.
 - a. This involves every part of the machine, Chiller, Vytran...
4. Select home/zero for all the system that involves every motor
5. Select the program
 - a. For this tapering, it was selected a program for the combiner. In this case, the transition was 3:1; the bundle of fibers was around 510um of diameter and finishing with the PL around 175um of diameter. The transition was in 25m, having the smallest size constantly in

10mm to have space to cut. This part depends on the number of fibers, density, sizes, and materials. These parameters have not been reported in any paper and the best for us was to change the velocity to 0.65m/s (the tension) and the power 145W (temperature). With those parameters, you can get the uniform melting. This was repeated many times with different values obtaining some images likes the exposed in the thesis.

6. Align the system to put the capillary tube in the middle of the filament.
 - a. This is in the three axes (X,Y,Z) and here you will need two capillary tubes to align one mounting to the other one.
7. Remove the capillary tubes
8. Select the command to maintain the filament up after the process
9. Move the right motor two small steps
10. Select anti back slaws
11. Start the process without the capillary tube.
 - a. To eliminate dust in the filament, check the distances of the motors (to do not have problems with space and to know the length that it will increase). Change power.
12. Select the option to start a new tapering
13. Clean the external part of the bundle
14. Mount the bundle
15. Move the right motor two small steps
16. Select anti back slaws
 - a. Check the characteristics of this tapering (145W and 0.65m/s in this case)
17. Start the process
18. Remove the Photonic Lantern
19. Down the filament
20. Put the PL
21. Hold the PL
22. Move both motors to the same direction

23. Cut the PL

- a. In this case, there was not a especial machine to cut this device in the red line of the figure 3'. I tried many different forms to do it, the best one was to pull both sides, after to do a line with a diamond peak to start to pull one side slowly until it brakes.

24. Take pictures of the Photonic Lantern with the Vytran to rectify the result

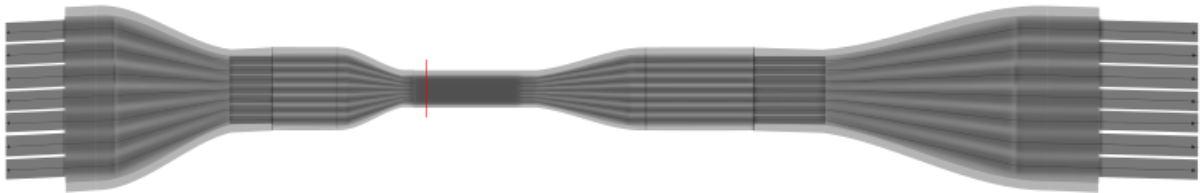


Figure 3' Second tapering with a red line to cut

This was the process to create it.

Details of a extended source with a PL

There are some issues to put the new device in a regular set up, fist the LED to use. In this thesis, there were two kinds of LEDs. One from ThorLabs that is used like a fluorescence lamp and the second one was the Luminus devices from Digi-Key Electronics with codes CBT-90-RX-L15-BN101, CBT-90-B-L11-J101, and CBT-90-G-L11-CM10. Those powerful LED from Luminus devices required high current and for that, we bought a Battery control module, EA Elektro-Automatik, PS 3016-10B, 1 output / s, $0 \rightarrow 16V$, 10A, 160W. For this kind of devices, there are problems with the current, it is important to isolate the system from the optical table. In addition, it has to be isolated from the heatsink, which has to be big with at least 1Kg for the heat due to the high current.

To understand the behavior of this kind of sources, it is important to characterize it. One example is the divergence that will affect the people working on those places (it has to be in a box) or in the creation of imaging to focus the light in a certain area. An example is with the ThorLabs LEDs the Maximum power was 2mW and with that, I could generate 0.15 uW in the output of the PL, by another hand, using the Powerful LEDs in one case I focused 52mW with an output of 0.30uW. Those issues appear depending on their characteristics. It is recommendable to do not use LED without the cover of flat, the divergence will be extremely high. The tools to focus the LED will depend on the LED that you prefer to use.

All the other aspect considered in the thesis like the sources of loses to consider and the position of the optical fibers to do the light sheet. On the other hand, the way to mount the PL is important to consider:

1. Do not have to twist the fiber
 - a. it has to be in a straight line
2. Remove coating of the end of the optical fibers
 - a. To cut it, to do not losses in the optical power
3. Put all the fibers together in a line
 - a. In this part, I mount the system in a rotatory mount, which can move x-axis and y-axis. I put a plate inside the mount to put the fibers there with tape.
 - b. It has to be in a precise way.
4. The MO has to have the same numerical aperture or higher than the optical fiber to collect the entire light.

Details of mounting a PL in a LSFM

In this case, to do the Light Sheet you will need a neutral density filter and a gadget to put a small mirror where the sample has to be, to send the light to the camera.

Having the mounting of the PL in a vertical way compared with the optical table. To determine the right position of the cylindrical lens, we have to rotate it until having something like figure 4', there, the cylindrical lens is orthogonal, so rotating it 90 degrees will leave the Cylindrical lens in the right position. However, the light sheet would not be in the same axis, to have just one LS, the gadget has to be implemented where the sample has to be, to see the front view of the LSs. Here you can rotate the optical fibers, the distance to collimate, the distance of the MO or illumination or the focusing to get the best LS. Another useful tool is the implementation of beads.



Figure 4' Cones of light with a PL with and orthogonal CL or without one.

Zebrafish immunostaining

We used 2dpf (days post-fertilization) zebrafish embryos of a transgenic line that has GFP protein expressed in all cell membranes (CAAX-GFP Tg). We performed an immunostaining against alfa-tubulin (microtubules) and tom20 (mitochondrial protein).

1. FIXATION: 2dpf (days post-fertilization) CAAX-GFP zebrafish embryos were dechorionated and fixed overnight in 4% PFA/PBS at 4 °C
2. PBS washes X3 5' each, gentle shaking
3. BLOCKING AND PERMEABILIZATION (triton is a detergent that permeabilizes cell membranes. Bovine serum albumin (BSA) is used as blocking reagent since it prevents unspecific binding of the antibodies):
 - a. PBST (PBS+0.3 TRITON) washes x4 15' each, gentle shaking
 - b. BLOCK SOLUTION (1% BSA in PBST) incubation for 2 hours, gentle shaking
4. STAINING:
 - a. PRIMARY ANTIBODY INCUBATION*: dilute at the desired concentration (8µg/ml) in BLOCK SOLUTION. Incubate overnight at 4°C, gentle shaking.
 - b. PBST (PBS+0.3 TRITON) washes over day (change every hour or so), RT gentle shaking.
 - c. SECONDARY ANTIBODY INCUBATION**: dilute at desired concentration (8µg/ml in BLOCK SOLUTION and incubate overnight at 4°C, gentle shaking, in the dark
 - PBS washes X3 5' each, RT gentle shaking. Ready to mount and image.

- *primary antibodies used:

- Anti- α -tubulin (mouse)
- Anti-TOM20 (rabbit)
- ****secondary antibodies used:**
 - Donkey-anti-mouse-Alexa532

Donkey-anti-rabbit-AbberiorSTAR635P

List of Tables

Table 1	Characteristics of a Light Sheet with a Laser and a LEDs.....	33
Table 2	The number of modes of each optical fiber with three different wavelengths, changing the diameter and the required values to calculate the number of modes. Some values took it from a commercial enterprise.	48
Table 3	Characteristics of the SMF 28 and the PL with a LED of 0.08675mm ² of area and 2.16mW of power. The last results are optimizing this PL in the output.	52
Table 4	Characteristics to do LS with a lase, LED and the novel illumination	65

List of Figures

Figure 1 Jablonski's diagram, transitions of energy to obtain fluorescence. The blue line is the level transition of the electron, it happens when the electron is irradiated with the excitation wavelength. The red line represent the non-radiative transition, which the electron lose energy without emitting a photon. The green line is the transition from an excited state to a lower state, emitting in a bigger wavelength than the excitation.....	6
Figure 2 a) Different fluorescence microscopy techniques, a) wide field: illuminating the entire sample with the wavelength of excitation. b) Confocal microscope: Focused the illuminated light in a point. c) LSM: the illumination is in one plane and the detection is in an orthogonal position with respect the illumination.	7
Figure 3 The illumination and detection in LSM must to be orthogonal due to the plane of focus in the sample.....	8
Figure 4 Types of illumination. In microscopy, the different types of illumination depend on the mounting of the set-up. a) The simplest system, one illumination and one detection an orthogonal plane. b) Two illuminations and one detection to have more light in the sample in the same section. c) Two illuminations and two detections. d) Illumination and detection with 45 degrees with respect of the horizontal.	9
Figure 5 The two axes of the CL. a) The beam is focused in the back focal plane of the MO, generating a collimated beam as a result. b) The axis does not affect the direction of the light and then it will be focused at the work distance.	11

Figure 6 Illumination part in a LSFM filled in the MO. a) Lateral view of the LS in the axis of the CL. b) Upper view, the opposite axis of the CL.....	13
Figure 7 Phenomena in a sample irradiated by a laser. a) Scattering, fluorescence, reflexion, other. b) Scattering. c) Fluorescence	14
Figure 8 Detection part composed by a microscope objective, a tube lens, filter of the emission wavelength and the camera.....	14
Figure 9 Point sources with diffraction (Airy pattern) separated by different distances. a) Resolved. b) Resolution limit. c) Unresolved	15
Figure 10 Mounting setup. The red line shows the capillary tube where is mounted the sample, the blue one to control the rotation and the green and yellow one to control the three axis X, Y, and Z.	17
Figure 11 Characteristics of the LS and Beads a) Cone of the focused beam without CL. b) beam with CL in the entire screen. c) Front view Light Sheet. d) Beads.	19
Figure 12 Maximum projection of two images of different distances.	20
Figure 13 The middle part of a cancer spheroid labeled with H2B-mCherry.....	21
Figure 14 Reconstruction of two spheroids in 3D. All of them are from the same sample in different points of view.	22
Figure 15 Maximum projection of the two spheroids.....	22
Figure 16 Finger pattern in a Michelson's Interferometer	25
Figure 17 Speckle patterns.....	25
Figure 18 A Light Sheet Fluorescence Microscope.....	26

Figure 19 Images of a zebrafish like a sample. a) The bright field in the same position as before one. b) With LSFM. c) Maximum projection of the sample's stack with LSFM.....	27
Figure 20 LUMINUS CBT-90 TE LEDs' Spectrum	29
Figure 21 Illumination part of a LSFM. a) Just collimating the light. b) Using a diaphragm. c) LED inside an optical fiber (CL-Cylindrical Lens).....	31
Figure 22 LSFM with incoherent light and a spatial filter (pinhole)	31
Figure 23 Image of the LS created with incoherent light. It is homogenous and the size is around 20 μm	32
Figure 24 The Optical fiber is composed of three different parts: core and cladding to generate the total internal refraction and the coating to protect the optical fiber.	34
Figure 25 Transversal section of optical fiber: the first one is with a core of 3 μm - size for single mode in around 480 μm , the second one is of 8 μm - single mode in 1550nm and multimode in visible light, the last one 50 μm -multimode for visible light and 1550.....	35
Figure 26 Parts of a Photonic lantern and elements	37
Figure 27. (Left) Transitions of a multimode to single modes. It could start since the number one to number 5 or vice versa. (Right) Schematic evolution of supermodes throughout the tapered transition of the PL. The inverse of the refractive index profile ($1/n$) vs. radius For the vertical axis, a comparison is made between transverse wavevectors (KT) of photons and energy of the electron (E) at different positions along with the tapered transition. [45].	40

Figure 28 The evolution of modes throughout a seven fiber photonic lantern. The red horizontal dashed lines indicate the core and cladding index of the final multimode core ($n_{co}=1.444$; $n_{cl}=1.4431$). (Right panel) Detail of the calculated modes supported by the photonic lantern at the multimode end. [42]..... 42

Figure 29 Tapering a) after the first one with the optical fibers without counting in the smallest section. b) The second one with a red line where it has to be cut. .. 43

Figure 30 The transition of the melting. In the left, there is just a bundle of fibers. There is a semi-fusion of the fibers in the image of the middle. The last one is a complete fusion. 44

Figure 31 Tapering of PLs. a) More power than the reduction of the fibers and low velocity. b) Correct transition. c) High velocity and high power. 45

Figure 32 Sources of losses. a) A bad cut of the PL. b) Front view of a bad cut. c) Reduction of the fiber with just six elements. d) Dust or residual material in the PL. 46

Figure 33 Photonic Lanterns made it with different kind of optical fibers a) SM450 ~ 3.4um core, b) SM800 ~5.6 core, c) SFM28 ~8um core and d) AFS105 ~105um core..... 47

Figure 34 The optical path of the LED light for the optical system..... 49

Figure 35 The blue graph shows the profile of the input light in the PL and the green one shows the output light of the PL. 50

Figure 36 Pictures of the output light a) Front side of the PL. b) Two images of the front side using different wavelengths. The first amplification is with around eleven

modes considering a green led with the peak in 530nm that it showed in table 2.

The second amplification is with a peak in 780nm having around six modes..... 51

Figure 37 LSFM with a PL for different wavelengths..... 54

Figure 38 Front view of the optical fibers. a) Seeing the focused plane and with magnification, b) CL with the axis in the horizontal plane, with respect to the table. c) CL in a vertical plane with respect to the table. In all the cases the light travels inside the cladding too..... 55

Figure 39 Characteristics of the new mounting. a) Lateral view of the focusing, b) and c) front view rotating the PL..... 56

Figure 40 The light sheet of the PL, in each image the focused plane was for a different line. a) Focused for the first one with a thickness of 6.169, b) the second one with 7.32 of thickness, c) 4.47 and d) 4.12..... 58

Figure 41 Light Sheet Fluorescence Microscope with both illumination systems 58

Figure 42 Images of a zebrafish egg, a) the first section is composed by the image of bright field, a section did it with fluorescence with the Laser and the maximum projection of the stack. In the other case, b) it is the same sequence, just adding the scattering imaging and in the last image removing the maximum projection of fluorescence, with was more noise than image. 60

Figure 43 Cancer Spheroids, a) Fluorescence image did it with laser b) scattering image did with a LED and the PL 61

Figure 44 Images of fish tail, a) with the PL producing fluorescence, b) fluorescence with the Laser, c) removing the filter of illumination to see fluorescence and scattering and d) removing all the filters. 62

Figure 45 Zebrafish tail, a) image using a Laser and b)) image using a LED with the Photonic Lantern. 63

Figure 46 Setup with different optical paths, the blue one is of the laser to do images, the blue blur optical part is of the alignment, the three colors come from the LEDs and it passes through the PL, and the yellow one is the detection wavelength that will depend on the source of light and the kind of imaging..... 63

Figure 47 The red images represent the tail of the fish a time exposure of 100ms, a)l image using a Laser and b) image using the PL with the LED, the blue images are with 1s of exposure time using c) the Laser and d) the PL with the LED..... 64

Figure 48 same section of the tail, a) scattering imaging, b) membrane, c) a low staining that with imaging processing can see something and d) nothing in the red channel. The illumination has a filter with different bandwidth of the detection to do not see interference, this image show that the filter works well and the staining no. 66

Figure 49 Images of the zebra fish tail, each image shows different structures, a) the one produced with scattering, b) membrane, c) tubulin, d) mitochondrion, e) the superposition of all the channels..... 67

Figure 50 Cross section of a part of the Figure 49, since a to d there were added channels a) mitochondrion, b) tubulin, c) scattering and the last added was d) membrane. 67

Figure 51 Image of a zebrafish with 48h hours with four different structures: membrane, tubulin, mitochondrion and scattering. The black circle shows a zoom of a specific section. The blue circle shows that it is possible to select just one part

of the sample to have a zoom of the zones that it is not possible to see like the green circle. In the super position of the structures, the color are combine producing with parts..... 68

Figure 52 Images of zebrafish with 48h after birth, the left image show a maximum projection scanning since a lateral view, and the right image the scanning was since the head. 69

Bibliography

- [1] W. A.J.M., "Wollman A.J.M., Nudd R., Hedlund E.G., Leake M.C. "From animaculum to single molecules: 300 years of the light microscope." *Open Biology*, 5, (2015). DOI: 10.1098/rsob.150019".
- [2] "Misha B Ahrens, Michael B Orger, Drew N Robson, Jennifer M Li & Philipp J Keller "Whole-brain functional imaging at cellular resolution using light-sheet microscopy." *Nature Methods*, 10(1), pages 413–420 (2013).".
- [3] "Per U, Nobuyuki T. "Improved Pathological Examination of Tumors with 3D Light-Sheet Microscopy." *Trends in Cancer*. 4(5), 337-341 (2018).".
- [4] " A. Jablonski "Efficiency of Anti-Stokes Fluorescence in Dyes" *Nature* 131, 839–840 (1933)".
- [5] "F. Rost [Encyclopedia of Spectroscopy and Spectrometry] Elsevier (1999)".
- [6] "Melanie M. F., Judith L., Jody L. S., Claire M. B. "Live-cell microscopy – tips and tools" *Journal of Cell Science* 122: 753-767; (2009) doi: 10.1242/jcs.033837".
- [7] "Jennifer C. Waters, [Methods in Cell Biology] Academic Press Vol. 114, 125-150, (2013) <https://doi.org/10.1016/B978-0-12-407761-4.00006-3>".
- [8] "E. H. K. Stelzer, "Light-sheet fluorescence microscopy for quantitative biology." *Nat. Methods* 12, 23–26 (2014).".

- [9] "J. Huisken, J. Swoger, F. Del Bene, J. Wittbrodt, and E. H. K. Stelzer, "Optical sectioning deep inside live embryos by selective plane illumination microscopy," *Science* 305, 1007 – 1009 (2004).".
- [10] "Peter A. "Light sheet fluorescence microscopy: a review" *journal of histochemistry and cytochemistry: official journal of the Histochemistry Society* vol. 59, 2 129-38. (2011).".
- [11] "Reynaud, Emmanuel G et al. "Light sheet-based fluorescence microscopy: more dimensions, more photons, and less photodamage" *HFSP journal* vol. 2, 5, 266-75, (2008).".
- [12] "F. Pampaloni, N. Ansari, P. Girard, and E. H. K. Stelzer, "Light sheet-based fluorescence microscopy (LSFM) reduces phototoxic effects and provides new means for the modern life sciences," *Adv. Microsc. Tech. II* 8086, 80860Y (2011).".
- [13] "Philipp J K, Francesco P, Ernst HK S, "Life sciences require the third dimension" *Current Opinion in Cell Biology*, V. 18- 1, P. 117-124, (2006).".
- [14] "Marjolein B. M. Meddens, Sheng Liu, Patrick S. Finnegan, Thayne L. Edwards, Conrad D. James, and Keith A. Lidke, "Single objective light-sheet microscopy for high-speed whole-cell 3D super-resolution," *Biomed. Opt. Express* 7, 2219-2236 (2016)".

- [15] "P. J. Verveer, J. Swoger, F. Pampaloni, K. Greger, M. Marcello, and E. H. K. Stelzer, "High-resolution three-dimensional imaging of large specimens with light sheet-based microscopy, " *Nat. Methods* 4 , 311 – 313 (2007).".
- [16] "P. J. Keller, A. D. Schmidt, A. Santella, K. Khairy, Z. Bao, J. Wittbrodt, and E. H. K. Stelzer, "Fast, high-contrast imaging of animal development with scanned light sheet-based structured-illumination microscopy, " *Nat. Methods* 7 , 637 – 642 (2010)".
- [17] "R. M. Power and J. Huisken, "A guide to light-sheet fluorescence microscopy for multiscale imaging, " *Nat. Methods* 14, 360 – 373 (2017).".
- [18] "Fei, P. et al. Cardiac Light-Sheet Fluorescent Microscopy for Multi-Scale and Rapid Imaging of Architecture and Function. *Sci. Rep.* 6, 22489; doi: 10.1038/srep22489 (2016).".
- [19] J M Girkinand, M T Carvalho, "The light-sheet microscopy revolution" *Journal of Optics.* V 20-5, (2018)..
- [20] E. G. Reynaud, J. Peychl, J. Huisken, and P. Tomancak, "Guide to light-sheet microscopy for adventurous biologists," *Nat. Methods* 12 , 30 – 34 (2014)..
- [21] J. Swoger, M. Muzzopappa, H. López-Schier, and J. Sharpe, "4D retrospective lineage tracing using SPIM for zebrafish organogenesis studies," *J. Biophoton.* 4, 122 – 134 (2011).

- [22] T. Ichikawa, K. Nakazato, P. J. Keller, H. Kajiura-Kobayashi, E. H. K. Stelzer, A. Mochizuki, and S. Nonaka, “ Live imaging of whole mouse embryos during gastrulation: migration analyses of epiblast and mesodermal cells, ” PLoS ONE 8 ,(2013).
- [23] Anna K., Michaela M., Michael W., Jan H. “Multilayer mounting enables long-term imaging of zebrafish development in a light sheet microscope” Development 139: 3242-3247; (2012) doi:10.1242/dev.082586.
- [24] L. Breimann, F. Preusser and S. Preibisch, “Light-microscopy methods in C. elegans research” Systems biology of model organisms 13, 82-92 (2019).
- [25] "Omar E. Olarte, Jordi Andilla, Emilio J. Gualda, and Pablo Loza-Alvarez, "Light-sheet microscopy: a tutorial," Adv. Opt. Photon. V. 10, 111-179 (2018)".
- [26] "B. E. A. Saleh, M. C. Teich [Fundamentals of Photonics] John Willey & Sons, Inc. (1991)".
- [27] "E. Hecht [Optics] Addison Wesley, Fourth Edition (2002)".
- [28] "J. R. Reitz, F. Milford, R. Christy [Foundations of Electromagnetic Theory] Pearson; 4th edition (2008)".
- [29] "A.E. Siegman [Lasers] University Science Books (1986)".
- [30] R. Dändliker “The concept of modes in optics and photonics,” SPIE Vol. 3831, 193-198 (2000).

- [31] "Agrawal G.P. [Optics in Our Time]. Springer, Cham (2016)".
- [32] "Marazuela, M. & Moreno-Bondi, M. "Fiber-optic biosensors – an overview" Analytical and Bioanalytical Chemistry 372, 664 (2002) <https://doi.org/10.1007/s00216-002-1235-9>".
- [33] "D. Y. Tang, H. Zhang, L. M. Zhao and X. Wu, "Vector soliton fiber lasers," 2009 14th OptoElectronics and Communications Conference, Vienna, 2009, pp.1-2. doi:10.1109/OECC.2009.5222567".
- [34] "Ivan P. K., Tingye L. and Alan E. W. [Optical Fiber Telecommunications: Systems and Networks] Academic Press, 6th Edition. (2013) <https://doi.org/10.1016/C2011-0-06882-5>".
- [35] "S. G. Leon-Saval, T. A. Birks, J. Bland-Hawthorn, and M. Englund, "Multimode fiber devices with single-mode performance," Opt. Lett. 30, 2545-2547 (2005)".
- [36] "David B. Mortimore and John W. Arkwright, "Monolithic wavelength-flattened 1 X 7 single-mode fused fiber couplers: theory, fabrication, and analysis", Applied Optics, 30, 6 (1991)".
- [37] "B. Wang, E. Mies, "Wavelength and Polarization Dependences of Fused Fiber Couplers" Journal of Lightwave Technology, 29, 3, (2011)".
- [38] "T. A. Birks, I. Gris-Sánchez, S. Yerolatsitis, S. G. Leon-Saval, and R. R. Thomson "The photonic lantern", Advances in Optics and Photonics 7, (2015)".

- [39] "S. G. Leon-Saval, "Photonic Lantern: harnessing multimode photonics for optical communications," in Asia Communications and Photonics Conference, OSA Technical Digest (2017)".
- [40] "T. A. Birks, B. J. Mangan, A. Díez, J. L. Cruz, and D. F. Murphy, "“Photonic lantern” spectral filters in multi-core fibre," Opt. Express 20, 13996-14008 (2012)".
- [41] "A. Arriola, D. Choudhury, and R. R. Thomson "New generation of photonic lanterns for mid-IR astronomy", Advances in Optical and Mechanical Technologies for Telescopes and Instrumentation, 915116 (2014); <https://doi.org/10.1117/12.2056526>".
- [42] " Sergio G. Leon-Saval, Alexander Argyros and Joss Bland-Hawthorn “Photonic lanterns” Nanophotonics 2 (5-6), (2013)".
- [43] "T. Kato "On the Adiabatic Theorem of Quantum Mechanics". Journal of the Physical Society of Japan. 5 (6): 435–439 (1950).".
- [44] "Teufel, Stefan. "A note on the adiabatic theorem without gap condition." Letters in Mathematical Physics 58.3 (2001): 261-266.".
- [45] "S. G. Leon-Saval, A. Argyros, J. B. Hawthorn, “Photonic lanterns: a study of light propagation in multimode to single-mode converters” OPTICS EXPRESS 18, 8 (2010).".

- [46] "D. Noordegraaf, P. M. W. Skovgaard, M. D. Maack, J. Bland-Hawthorn, R. Haynes, J. Lægsgaard "Multi-mode to single-mode conversion in a 61 port Photonic Lantern" OPTICS EXPRESS 18, 5 (2010)".
- [47] "D. Noordegraaf, P. M. W. Skovgaard, R. H. Sandberg,1 M. D. Maack, J. Bland-Hawthorn, J. S. Lawrence, J. Lægsgaard2 " Nineteen-port photonic lantern with multimode delivery fiber" OPTICS EXPRESS 37, 4 (2012)".
- [48] "Ibrahim Ozdur, Paul Toliver, Anjali Agarwal, T. K. Woodward "Free-space to single-mode collection efficiency enhancement using photonic lanterns" OPTICS EXPRESS 38, 18 (2013)".
- [49] "B. Wang, E. Mies "Review of Fabrication Techniques for Fused Fiber Components for Fiber Lasers" SPIE Photonic West '09 (2009)".
- [50] "Universitat de Barcelona, JOptics, 'optical fibers' (2010) DOI: 10.1344/401.0000000050".
- [51] "E. P. Goodwin and J. C. Wyant, "Field Guide to Interferometric Optical Testing", SPIE Press, Bellingham, WA (2006).".
- [52] "Jeff W. L. & José-Angel C. "Fluorescence microscopy" Nature Methods Vol 2, 910–919 (2005)".
- [53] "John L., Hwee K. L., Weimiao Y. and Sohail A." Light Sheet Fluorescence Microscopy (LSFM); Past, Present and Future." The Analyst, 139;19 (2014) DOI: 10.1039/C4AN00624K".

- [54] C. GM, *The Cell: A Molecular Approach.*, Sunderland: Sinauer Associates, 2000.
- [55] " B. Julien, T. Hwa-Yaw, G.Tom, C. Xin, J. Pun, Chi-Fung, W. Jian & L. Po-Heng
"Ultra-fast polymer optical fibre Bragg grating inscription for medical devices,"
Light: Science & Applications. 7, (2017). 10.1038/lsa.2017.161."
- [56] "N. Rogério, B. Lucia, M. Carlos, O. Roberson & H. Jamshid. "Optical filtering in
plastic optical fibers." *International Conference on Transparent Optical Networks*. 1-
4. (2013). 10.1109/ICTON.2013.6603054."
- [57] "R. R. Thomson, T. A. Birks, S. G. Leon-Saval, A. K. Kar, and J. Bland-Hawthorn,
"Ultrafast laser inscription of an integrated photonic lantern," *Opt. Express* 19, 5698–
5705 (2011)."